In situ Sulphur Isotope Study of the Prairie Creek Deposit, Southern Mackenzie Mountains, Northwest Territories: Deciphering the Conundrum of Three Deposit Styles in One

B.E. Taylor
Geological Survey of Canada, 601 Booth Street, Ottawa, ON, K1A 0E8
Bruce.Taylor@NRCan-RNCan.gc.ca

S. Paradis
Geological Survey of Canada, 9860 West Saanich Road, Sidney, BC

H. Falck
Northwest Territories Geoscience Office, Yellowknife, NT

B. Wing
Department of Earth and Planetary Sciences, McGill University, Montreal, QC

Abstract

The Prairie Creek district in the southern MacKenzie Mountains (Northwest Territories) includes base metal sulphide occurrences of three different styles: Mississippi Valley-type (MVT), stratabound replacement sulphide, and quartz-carbonate-sulphide veins. The Prairie Creek Zn-Pb-Ag deposit, itself, is comprised of two of these styles of mineralization, quartz-carbonate-sulphide veins and stratabound replacement base metal lenses. Discerning the relationship, if any, between these styles of mineralization may help develop exploration strategies. Sulphur isotope analyses are reported for 14 representative sulphide samples, including 12 of the stratabound replacement style, 1 vein sample, and 1 sample from an MVT occurrence, and compared to previously reported data, to characterize the isotopic compositions and states of equilibrium. We utilized a micro (in situ laser-assisted fluorination) high-spatial resolution analytical technique to document isotopic compositions of minerals within their textural context. The preliminary results of 214 individual analyses and the textural context of analyses in several selected samples are documented in this report. We hoped to uncover any connections between the three styles of mineralization, including their likely temperatures of formation and any isotopic gradients that would indicate paleo-hydrothermal flow.

Recommended citation

Taylor, B.E., Paradis, S., Falck, H., and Wing, B., 2015. In situ sulphur isotope study of the Prairie Creek deposit, southern Mackenzie Mountains, Northwest Territories: deciphering the conundrum of three deposit styles in one, *in* Paradis, S., ed., Targeted Geoscience Initiative 4: sediment-hosted Zn-Pb deposits: processes and implications for exploration; Geological Survey of Canada, Open File 7838, p. 96-133. doi:10.4095/296328

The overall range of $\delta^{34}S$ for stratabound replacement pyrite, sphalerite and galena was found to be large, ca. 16 ‰, but the distributions of $\delta^{34}S$ for pyrite and sphalerite are more restricted (1σ = 1.23 and 1.56 ‰, respectively), and less restricted for galena (1σ = 4.64 ‰). Analyses from an MVT sample from the Root River Formation, in which pyrite rims vugs in sparry dolomite, suggest that this style of mineralization may be unrelated to the stratabound replacement sulphides. The $\delta^{34}S$ of vein pyrite (from concentrate) corresponds rather well to pyrite from the stratabound replacement sulphides, and a similar relationship exists for galena. The similarity of sulphur isotope systematics for both veins and stratabound sulphides (including pyrite, sphalerite and galena) suggests a relationship between these two styles of mineralization, despite the fact that published Pb isotope investigations argue for separate origins (Paradis, 2007). The veins, or vein-related flow paths, may have acted as fluid conduits at various times, first as conduits for the fluids ($\delta^{34}S \approx 23$ ‰) that formed the stratabound lenses, and again at later time for the quartz-carbonate-sulphide veins. The presence of a principal vein, and its contained sulphide abundance, may constitute a guide for stratabound replacement sulphides at depth.

Isotopic variance on the millimetre-scale was such that average $\delta^{34}S$ values proved more practical for estimating temperatures of formation. However, isotopic disequilibrium was found to be common, and estimated isotopic temperatures are considered approximate at best. Our high-spatial resolution data suggest caution when interpreting sulphur isotope geothermometry in similar situations; whole-rock analysis may mask important variations. Estimates of formation temperatures for the stratabound bodies fell within the range of ca. 170-250°C. Veins appear to reflect similar, but perhaps a bit higher temperatures of formation. The principal stratabound sulphide lens (SD1) appears to record a variation in temperature, from higher values towards the centre and the main quartz-carbonate-sulphide vein, and cooler values towards the margins of the sulphide lens.

Introduction

The Prairie Creek deposit (61°33'11.6" N, 124°47'33.2" W; previously known as the Cadillac deposit), the largest carbonate-hosted Zn-Pb-Ag deposit in the southern Mackenzie Mountains, is situated in Silurian-Devonian carbonates on the edge of Mackenzie Platform, at the margin of the shale-dominated Selwyn Basin (Figure 1). Three styles of mineralization, classic Mississippi Valley-type (MVT), stratabound replacement sulphide (SRS), and quartz-carbonate-sulphide veins, characterize the Prairie Creek district. The latter two styles have been the focus of mineral exploration. The deposit currently contains ‘measured plus indicated’ resources of 3.7 Mt (vein-related) of 11.3% Zn, 12.4% Pb, 0.43% Cu and 202 g/t Ag and 1.281 Mt (stratabound) of 10.5% Zn, 6.1% Pb, and 65 g/t Ag (AMC Mining Consultants, Canada, 2012). Paradis (2007) provides a brief summary of exploration and mining history, from its first-mention in 1928 to 2007.

Paradis (2007) presented preliminary C, O, S, Sr, and Pb isotope data on samples from the contrasting mineralization styles in the Prairie Creek district, and suggested that SRS formed from bacterially-reduced seawater sulphate (BSR), as a replacement of carbonate units, along a basin margin, similar to interpretations of stratabound sulphide deposits in the Selwyn Basin, Yukon by Goodfellow and Lydon (2007). Vein sulphides were thought to be of a different origin, derived from basement fluids driven along deep faults (Paradis, 2007).

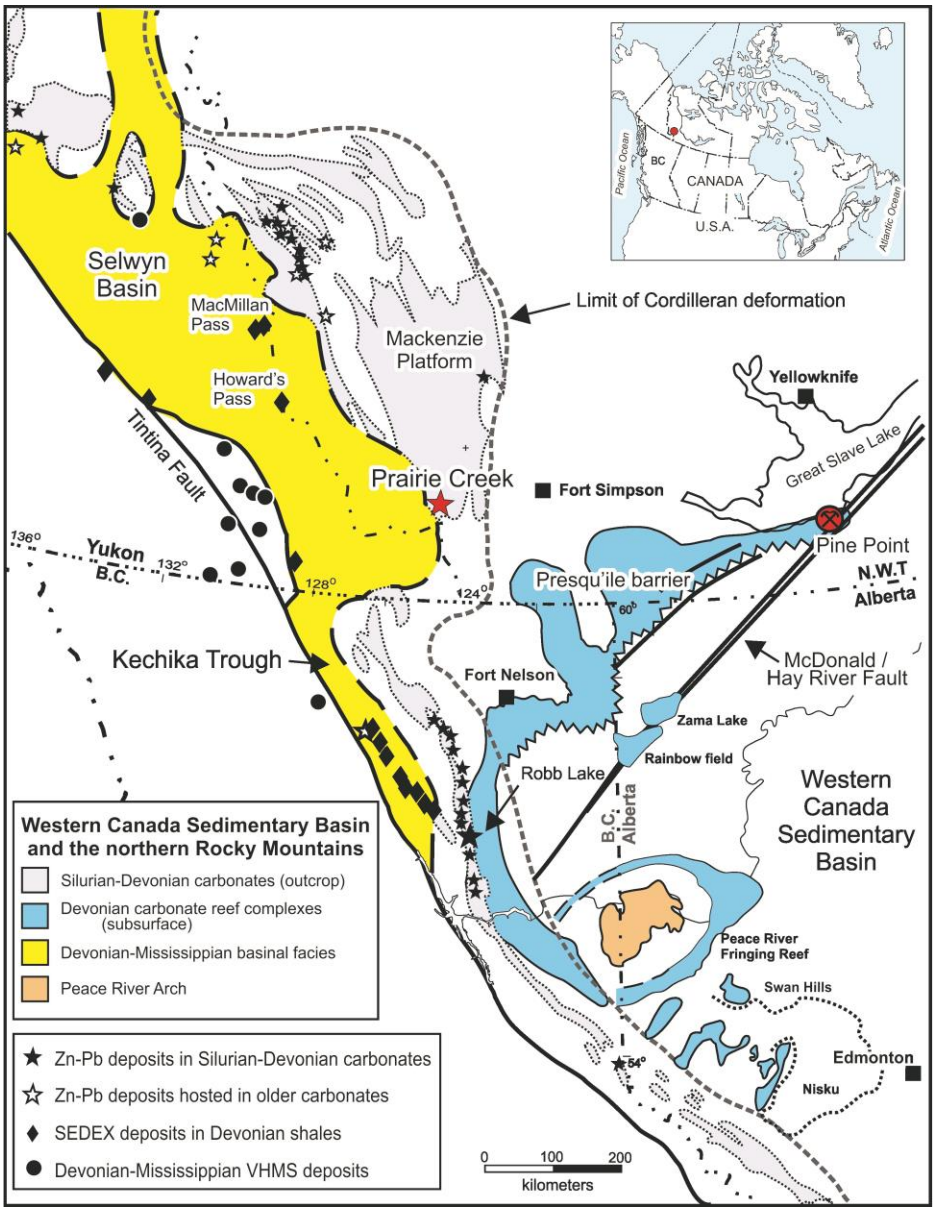

Figure 1. Regional map showing the location of the Prairie Creek deposit (red star), west of Fort Simpson, within the Mackenzie Mountains and carbonate rocks of the Mackenzie Platform (adapted from Paradis, 2007, and references therein). Note the association of deposit type with geologic terrane. Also shown is the location of the well-known Pine Point (MVT-style) deposit.

Geological Setting and Mineralization

Geological details of the Prairie Creek area are given by Morrow and Cook (1987), who sub-divided the Paleozoic strata into (bottom to top): 1) Sunblood Platform, 2) Mount Kindle-Root River Assemblage, 3) Prairie Creek Assemblage, and 4) Funeral-Headless Assemblage. The second subdivision, the Mount Kindle-Root River Assemblage is of principle relevance to the host strata of the Prairie Creek deposit. Paradis (2007, p.5) succinctly described the Assemblage as follows:

> "The Late Ordovician to Devonian Mount Kindle-Root River Assemblage consists of the Whittaker, Road River, and Root River formations. The Mount Kindle Formation, which is the shallow water reefal facies equivalent of the deeper water Whittaker Formation, is not present in the Prairie Creek area. Morrow and Cook (1987) divided the Whittaker Formation into three lithofacies: 1) a middle to upper Ordovician dark grey silty and sandy limestone (muOw1), 2) a middle to upper Ordovician fine-grained quartzite (muOw2), and 3) an upper Ordovician to Silurian laminated dark grey finely crystalline dolostone (OSw3), which hosts the stratabound sulphide mineralization at Prairie Creek. The lithofacies OSw3 has been subdivided into 7 subunits in the Prairie Creek deposit area by geologists of San Andreas Resources Corporation. The Silurian-Devonian Road River Formation comprises a sequence of graptolite-bearing shale and argillaceous bioclastic, shaly dolostone conformably overlying the Whittaker Formation. West of Prairie Creek, the Road River Formation thickens considerably in excess of 1000 m, and passes conformably upward into the Vera Formation. Eastward, in the Prairie Creek area, the Road River Formation thins to 170 m and is conformably overlain by the Cadillac and Root River formations. The Silurian Root River Formation is believed to be the shelf equivalent of the basinal facies of the Cadillac Formation. It consists of light grey, vuggy, micritic dolostone."

The history of structural deformation in the Prairie Creek district bears on the occurrence of both stratabound and vein style mineralization. In the area of the Prairie Creek deposit, north-south trending faults and fold axes have resulted in exposure of windows of Road River shale, cored by dolostones of the Upper Whittaker Formation, along the core of the Prairie Creek anticline. The anticline is doubly-plunging, with its axes plunging northward and southward from the mine site. The Prairie Creek anticline is structurally bounded to the east by the Prairie Creek Fault and to the west by the Gate Fault (Figure 2). These structures are presently north-south striking, west-dipping (65-90°) reverse faults that could have been originally normal faults (Earls, 1995; Fraser, 1996). The Prairie Creek Fault is a steeply dipping reverse fault with a thickness up to 40 m and a displacement of 1500 m (Morrow and Cook, 1987). Earls (1995) suggested that the Prairie Creek Fault might have initially been a west-side down, normal fault

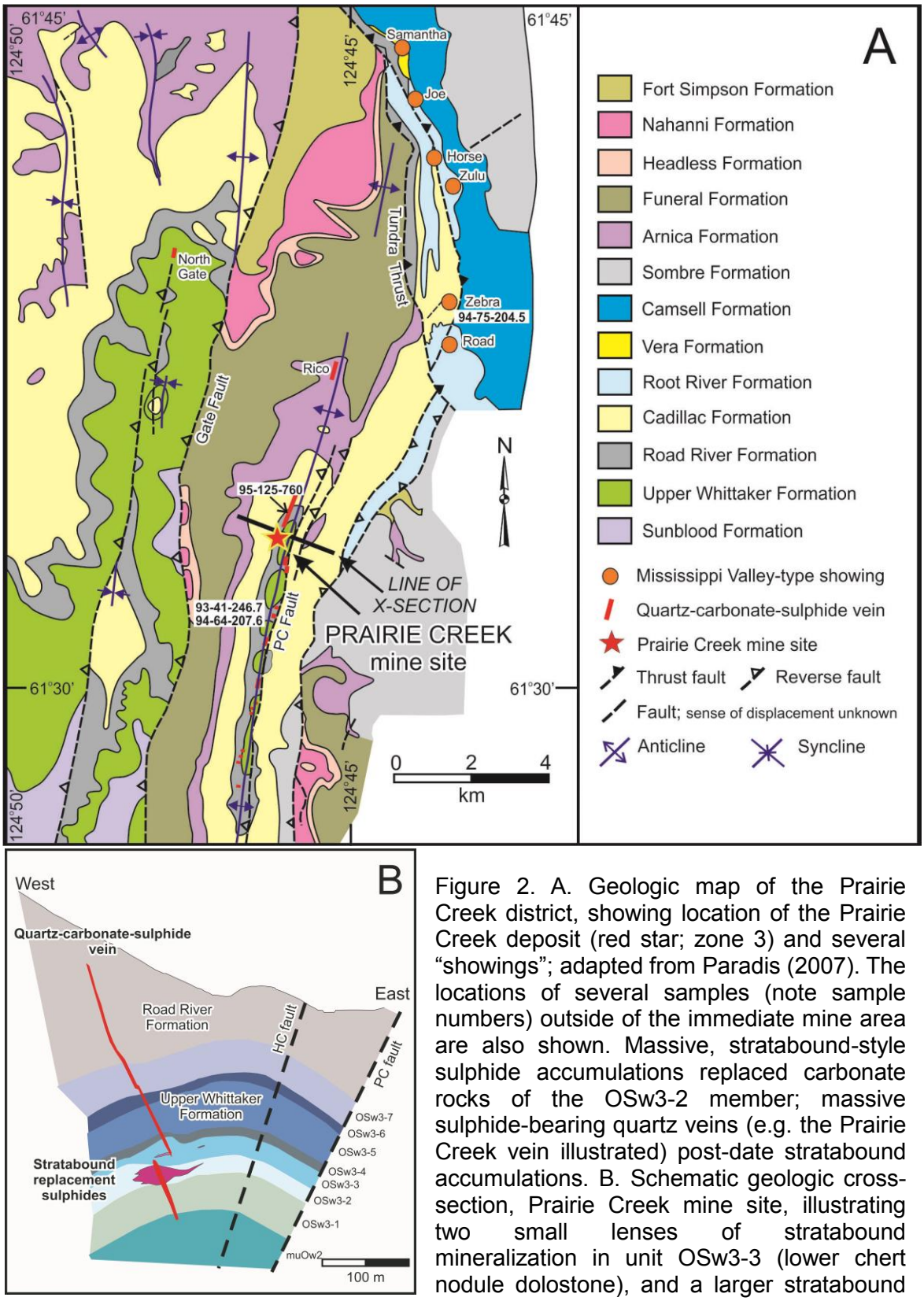

Figure 2. A. Geologic map of the Prairie Creek district, showing location of the Prairie Creek deposit (red star; zone 3) and several "showings"; adapted from Paradis (2007). The locations of several samples (note sample numbers) outside of the immediate mine area are also shown. Massive, stratabound-style sulphide accumulations replaced carbonate rocks of the OSw3-2 member; massive sulphide-bearing quartz veins (e.g. the Prairie Creek vein illustrated) post-date stratabound accumulations. B. Schematic geologic cross-section, Prairie Creek mine site, illustrating two small lenses of stratabound mineralization in unit OSw3-3 (lower chert nodule dolostone), and a larger stratabound lens in unit OSw3-2 (mottled dolostone) of the Upper Whittaker Formation; the section is located in A, above.

related to the formation of the Prairie Creek Embayment (see Morrow and Cook, 1987). Reactivation and reversal of movement would have occurred during the compressional event associated with the Laramide Orogeny.

Sulphide mineralization, as previously noted, occurs in the Prairie Creek district in three distinct styles: (1) SRS (likened to Irish type deposits: Earls, 1995; Findlay, 2000), which have replaced dolostone of the Upper Whittaker Formation; (2) quartz-carbonate-sulphide veins associated with the Prairie Creek fault, the fold axis of the Prairie Creek anticline, and other veins that cross-cut lower Paleozoic strata along 16 km of the exposed core of the Prairie Creek anticline; and (3) classic MVT sulphides that comprise open-space filling in vuggy shallow-water, shelf carbonates of the Silurian Root River Formation. Styles (1) and (2) have been the focus of mineral exploration.

Evidence of mineralization along some 16km of the north-south trending Prairie Creek fault, plus SRS up to 28m thick that occur discontinuously along a strike length of 3 km of the fault without surface expression, raise the need for exploration criteria. Understanding the origin(s) of the multi-faceted Prairie Creek deposit and various, broadly similar sulphide occurrences in the area, and their geologic controls, may provide essential knowledge for exploration. Are the three styles of sulphide occurrences related, i.e. are they textural/structural manifestations of the same mineralizing event, or do they have a distinct timing and origin? Initial sulphur isotope analyses reported by Paradis (2007) for samples of the vein, SRS, and MVT occurrences suggest that the MVT sulphides may be distinguished by having slightly lower $\delta^{34}S$ values (by ca. 8‰) relative to similar modes of analyses from the vein- and SRS. Strontium isotope ratios of calcite and dolomite from (14) samples of SRS, (3) samples of quartz-carbonate-sulphide veins, and (4) samples of MVT, in addition to (27) samples of host dolostone reported by Paradis (2007), exhibit a large range in values, and were noted to be markedly radiogenic. In particular, two samples of quartz-carbonate-sulphide veins plot at the upper end of the range, and have strontium isotope ratios as high as 0.7239 (Paradis, 2007).

The above observations suggest that mineralizing hydrothermal fluids were deeply sourced and had previously reacted with older crystalline rocks (Paradis, 2007). Lead isotope ratios, however, clearly distinguish sulphide minerals from vein and SRS mineralization on plots of $^{207}Pb/^{204}Pb$ or, $^{208}Pb/^{204}Pb$ vs. $^{206/204}Pb$. Stratabound replacement sulphides have $^{206}Pb/^{204}Pb$ and $^{207}Pb/^{204}Pb$ ratios that plot as an elongate group of data points primarily below the “shale curve” of Godwin and Sinclair (1982), but extending to intersect this growth curve at ca. 420 Ma. Paradis (2007) inferred a similar age for both the Prairie Creek SRS and the Devonian SEDEX deposits of the Selwyn basin. In contrast, the markedly different trend of Pb-isotope ratios for the quartz-carbonate-sulphide veins, which intersects the shale curve at ca. 250 Ma., i.e. about the Permian-Triassic transition, may indicate an age of formation different from that of the SRS

(Paradis, 2007). Without an absolute age determination, this possibility remains unproven, but if the quartz-carbonate-sulphide veins are younger than the SRS, then Pb-bearing fluids must have flowed through the vein-hosting structures at a later (post-replacement) time. In addition, the Prairie Creek fault, which is parallel in trend to the principal quartz-carbonate-sulphide vein (Figure 3), and perhaps other, vein-hosting faults, may have been re-activated during the Laramide Orogeny (Late Cretaceous; 70-80 Ma ago) as previously noted (see Morrow and Cook, 1987; Earls, 1995). In short, vein and SRS are not co-genetic. But, could they, nevertheless, be related?

Evidence necessary to better characterize the Prairie Creek deposit and determine its origin, state of sulphur isotope equilibrium and correct sulphide paragenesis, and possible paleo-thermal indicators of fluid flow, is locked within the sulphur isotope systematics of the sulphide minerals. We report on the sulphur isotope composition of sulphide minerals determined in their textural context by in situ methods. In situ, sulphur isotope analysis provides a unique means by which to address the unanswered question of whether multiple or single sources of sulphur (and/or fluids), or marked temperature contrasts were required to form the Prairie Creek deposit. Answers to these questions may provide a tool for regional exploration.

Sample Selection and Analytical Considerations

Fourteen samples were selected for the first phase of this study: 12 examples of SRS, and one example each of vein and MVT sulphides. Analytical work on an additional 28 samples is nearing completion. Sampled drillhole locations are shown in Figure 3. Samples are numbered with the drillhole number followed by drillhole depth (e.g. sample PC93-23-249.5 is from drillhole 93-23, and from a depth of 249.5 m. Sample descriptions, including sulphide mineral assemblages, for the 14 samples of phase I are presented in Appendix 1. Analytical work on an additional twenty eight samples is currently being completed that will extend the sample distribution throughout the Prairie Creek district.

In situ sulphur isotope analysis of mineral grains in polished, 1.0 mm-thick rock wafers, were carried out by laser-assisted fluorination, using MILES (Beaudoin and Taylor, 1994; Taylor and Beaudoin, 1993), as modified in Taylor (2004a; 2004b) at the Geological Survey of Canada, Ottawa. Sulphur isotope analyses were restricted to pyrite, sphalerite and galena, emphasizing high spatial resolution in order to permit analysis of adjacent grains, or intra-grain zoning. The sample chamber was often loaded with more than one sample, plus a chip of the laboratory internal standard (sphalerite from Broken Hill, Australia). Cooling the sample chamber and samples to ca. -100° to -60°C minimized the possibility of cross-contamination. The fluorinating agent employed was purified F_2 at low pressure, produced following the method of Asprey (1976; see Taylor, 2004b). The resultant micro-gas samples of SF_6 (typically ca. 0.1-0.3 μmoles; micromoles) were purified cryogenically (variable temperature trap: Taylor, 2004b) and sealed in 6 mm pyrex tubes for subsequent analysis for $\delta^{32}S$ and

$\delta^{34}S$ in a Thermo MAT 252 Isotope Ratio Mass Spectrometer (IRMS; Geological Survey of Canada, Ottawa), or for $\delta^{32}S$, $\delta^{33}S$, $\delta^{34}S$ and $\delta^{36}S$ in a Thermo-Electron MAT 253 IRMS, Department of Earth and Planetary Science, McGill University, Montreal. Further sample purification via gas chromatography was carried out on selected samples at McGill University prior to mass spectrometry.

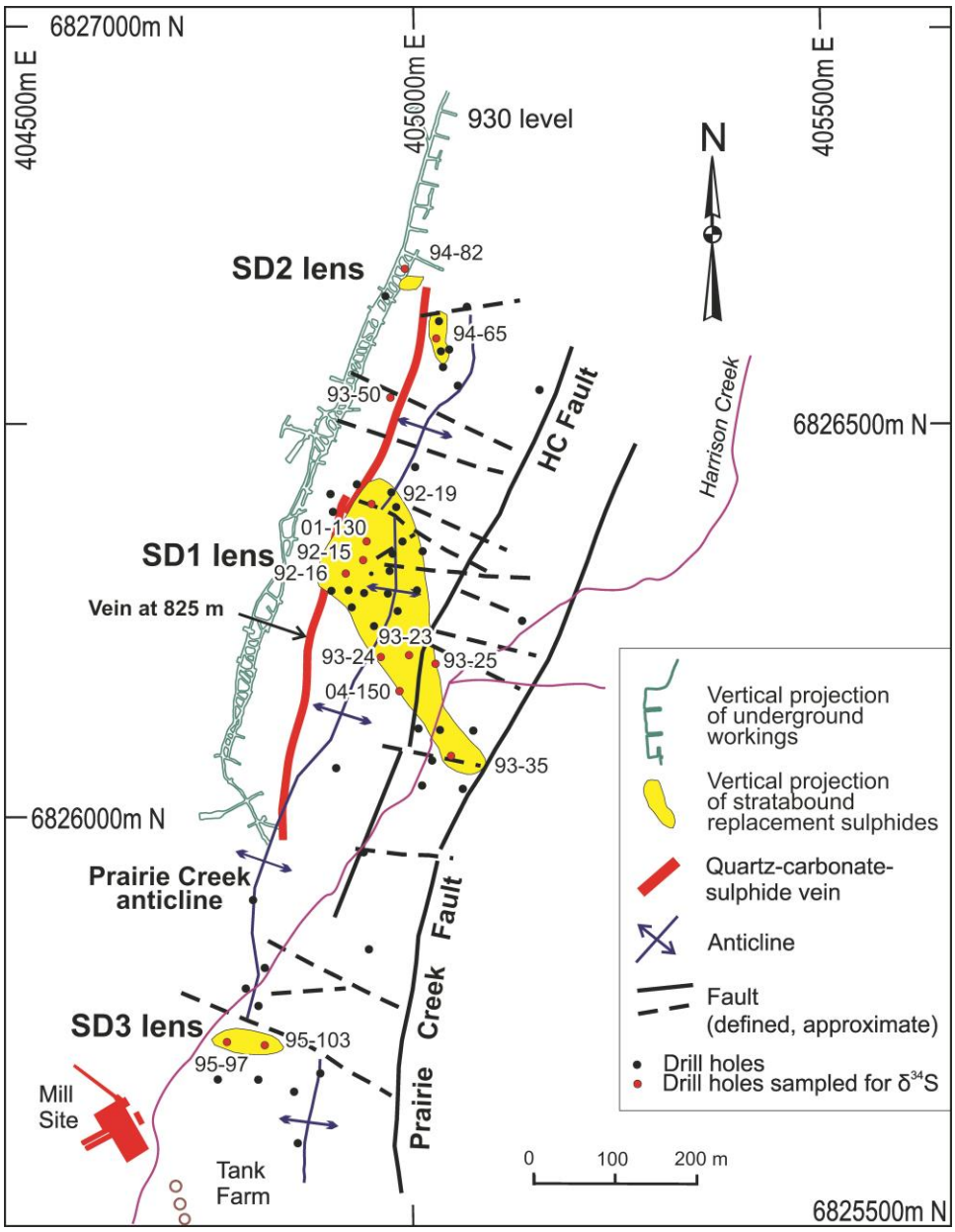

Figure 3. Map of the vicinity of the Prairie Creek minesite, showing vertical projections of stratabound sulphide occurrences, faults, fold axes, selected mine infrastructure, and the locations and identification numbers (e.g. 93-35) of sampled drillholes (see Appendices 1 and 2).

Gas chromatographic (GC) processing was found to be essential only for the accuracy of $\delta^{36}S$, since contamination of the ion beams by fluorocarbons is greatest at mass 131 SF_5^+; occasional exceptions do occur, however. The effect of beam contamination at mass 131 for samples not additionally purified via gas chromatography is very apparent from the variability and magnitude of results (in particular, $\delta^{36}S$). For in situ sampling, in particular (as opposed to grain samples of 1-3 mg), purification by gas chromatography should be routinely included as a 'best practice', for assurance.

Results/Data Analysis

The isotopic compositions of 214 in situ S-isotope analyses ($\delta^{34}S$, primarily, with some data for $\delta^{33}S$ and $\delta^{36}S$) of individual grains and/or analytical traverses within individual grains of pyrite, sphalerite, and galena are listed in Appendix 1. From 5 to 37 individual analyses were determined in each thin-section-sized polished wafer from examples of MVT, vein and SRS. Isotopic compositions are reported in the usual δ-notation ($\delta^{33}S$, $\delta^{34}S$, and $\delta^{36}S$), in per mil (‰) relative to V-CDT. Typical uncertainties are ≤0.2 per mil (2σ) for these in situ analyses, based on replicate in situ analyses of pure sphalerite from Broken Hill, Australia. Larger analytical uncertainties of in situ analyses of minerals can sometimes result using multi-mineral wafers due to reaction with other, unseen minerals beneath the sample surface, or reaction with adjacent minerals (although the reaction volume is minimized by use of a cold stage; Taylor, 2004a,b). The SF_6 gas samples produced in the process of in situ fluorination were on the order of 0.1 µmol, and were analyzed using a micro-volume inlet. Gas handling and potential variations in composition between aliquots of the reference gas during various analytical sessions at McGill University may have contributed additional uncertainty factors.

In Appendix 1, we report, in addition to $\delta^{33}S$, $\delta^{34}S$, and $\delta^{36}S$, values for $\delta^{33}S$ and $\delta^{36}S$, where, for example, $\delta^{33}S \equiv \delta^{33}S_{measured} - [(\delta^{34}S_{measured}/1000+1)^{0.515}-1] \times 1000$. The value of $\delta^{33}S$ provides a measure of deviation from the usual equilibrium mass-dependent fractionation, where $\delta^{33}S$ and $\delta^{34}S$ are related by a factor of 0.515. Marked deviations from this relationship, or '$\delta^{33}S$ anomalies', are typically ascribed to non-equilibrium, mass-independent fractionation (MIF) processes involving SO_2 in the Archean atmosphere, and primarily associated with Archean rocks older than ca. 2.2 Ga (e.g. Farquhar et al., 2010). Anomalous $\delta^{33}S$ values were not anticipated in this study, due to the age of the Prairie Creek deposit and host rocks; we focused on $\delta^{34}S$. However, all four sulphur isotopes were measured as a matter of course due to the arrangement of collectors in the Thermo-Electron MAT253 IRMS. We noted that several samples did deviate from the 0.515 linear relationship expected for mass-dependent sulphur isotope equilibrium, likely due to analytical issues rather than variance in S-source. Samples not GC-processed prior to mass spectrometry can be susceptible to errors in $\delta^{33}S$ and $\delta^{36}S$. The web-based stable isotope fractionation calculation tool of Beaudoin and Therrien (2004) facilitated ready calculation and comparison of the isotopic equilibration temperatures discussed in report.

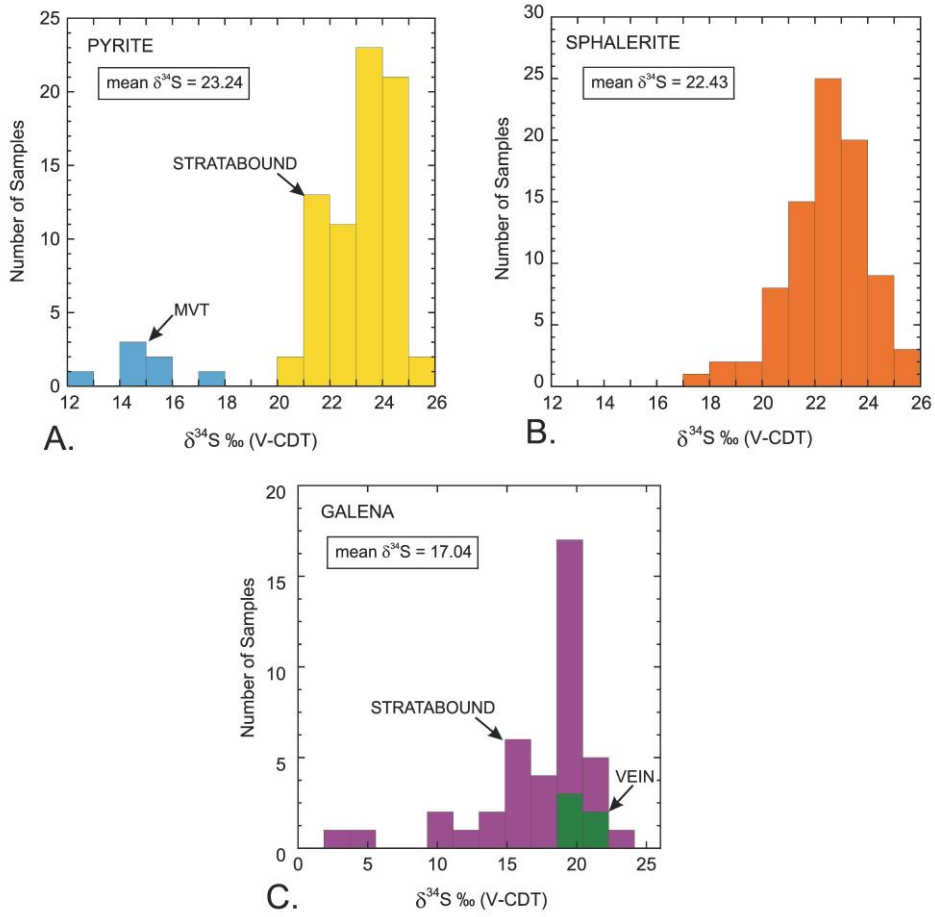

Figure 4. A. Histogram of in situ sulphur isotope analyses of pyrite illustrating a distinct population for the one sample of MVT sulphide occurrence analysed ($\delta^{34}S$ = ca. 14.7-17.1‰) from the Root River Formation. B. Histogram of results from in situ analysis of sulphur isotopes in sphalerite. A single population characterizes both stratabound and quartz-vein styles of sulphide occurrence; most analyses fall within a range of ca. 21-25‰. C. Histogram of in situ sulphur isotope analyses of galena. Two values for sample PC95-97-79.1 (stratabound sulphide in the OSw3-2 member) are strikingly anomalous. Similar to the data distributions for pyrite and sphalerite, a marked dominance occurs for one isotopic composition.

Histograms of $\delta^{34}S$ values for pyrite, sphalerite and galena from all in situ analyses are plotted and compared in Figure 4. The data for SRS dominate each of the histograms, whereas the ranges of $\delta^{34}S$ for each sulphide mineral are influenced by analyses from the MVT and vein samples. The ranges of $\delta^{34}S$ for SRS pyrite, sphalerite and galena were found to be large, up to ca. 16‰, whereas, the distributions of $\delta^{34}S$ for pyrite and sphalerite are rather restricted (σ =1.3 and 1.4‰, respectively), and less restricted for galena (σ = 4.5‰). Distributions for pyrite and galena (Figure 4) suggest two populations, although, in each case, the isotopically lighter results represent a single sample: pyrite ($\delta^{34}S$ = 14.7 – 17.1‰; PC94-75-204.5) in a sample from the Root River Formation, in which pyrite rims vugs in sparry dolomite and galena ($\delta^{34}S$ = 3.1

and 4.0‰; PC95-97-79.1) from the edge of massive sulphide in the Upper Whittaker Formation (Figure 3). Removal of data for these samples from the population in order to consider only stratabound occurrences, resulted only in a slight change in the mean value of $\delta^{34}S$ for sphalerite and galena of ca. 0.1 and 0.5‰, respectively.

The results of sulphur isotope analysis by oxidation to SO_2 of mineral concentrates from hand samples from the Prairie Creek district reported by Paradis (2007) differ in some respects from in situ analyses by fluorination reported here. The mean per mil fractionations (Δ) between pyrite and sphalerite and between sphalerite and galena for SRS ($\Delta_{pyrite\text{-}sphalerite}$: -2.08, and $\Delta_{sphalerite\text{-}galena}$: 1.64; Paradis, 2007) differ from those values reported here ($\Delta_{pyrite\text{-}sphalerite}$: 0.82, $\Delta_{sphalerite\text{-}galena}$: 5.09), and similarly for veins and MVT occurrences (although the data base of in situ analyses is small). Notably, the mean stratabound $\Delta_{py\text{-}sp}$; value reported by Paradis (2007) indicates a marked state of disequilibrium (i.e. it is a negative rather than a positive value). The reasons for this discrepancy require further investigation; isotopic variations on both local and district-wide scales may be involved. The nature of isotopic variation at the grain-to-grain scale is described below for several examples from the in situ analyses acquired in the present study.

The documentation of the textural environments of all in situ analyses carried out in this study requires more space than is practical for this report. All analyses are documented, however, in a separate Geological Survey of Canada Open File report (Taylor et al., in preparation); results and documentation of analyses in selected samples presented below provide examples of the textural-isotopic relationships encountered, as well as the apparent states of isotopic equilibrium (and implied paleo-temperature information) preserved. Traditional application of per mil isotopic fractionations between minerals for the estimation of temperatures of equilibration had often sought agreement for temperatures between three (or more) coexisting minerals. Multi-mineral isotopic equilibrium may not often be achieved in situations (e.g. as noted below) where hydrothermal replacement has occurred. Unfortunately, in the absence of agreement between three minerals constituting two co-existing pairs, the only guide to the accuracy of an isotopic temperature based on just one mineral pair is whether the result is ‘geologically reasonable’. Agreement with other examples from the same setting provides some assurance, if not confirmation. For the sake of consistency, we make use of the sulphur isotope fractionations determined by Kajiwara and Krouse (1971) to estimate the temperatures of formation of sulphide minerals in this study; comparison with several other fractionations determined by others for some of the mineral pairs suggest that those of Kajiwara and Krouse (1971) are sufficiently accurate for our purposes as we search for thermal gradients and compare the styles of mineralization in the Prairie Creek district.

The variation of values of $\delta^{34}S$ for individual, in situ analyses shown in Figures 5 to 11, suggests isotopic disequilibrium on a small scale, and raises several questions when calculating isotopic equilibration temperatures. Which point analyses should be used to construct an 'equilibrium mineral pair', or triplet (if possible)? Is it more prudent to calculate the average value in a sample for each mineral? The answers are not always straightforward. Here, we recognize the common state disequilibrium on the one hand, and attempt to make a 'best estimate' of equilibration temperature on the other hand, acknowledging that this estimate may have some uncertainty attached. The sample average and pair-wise per mil fractionations reported in Appendix 2 emphasize the difficulties at hand.

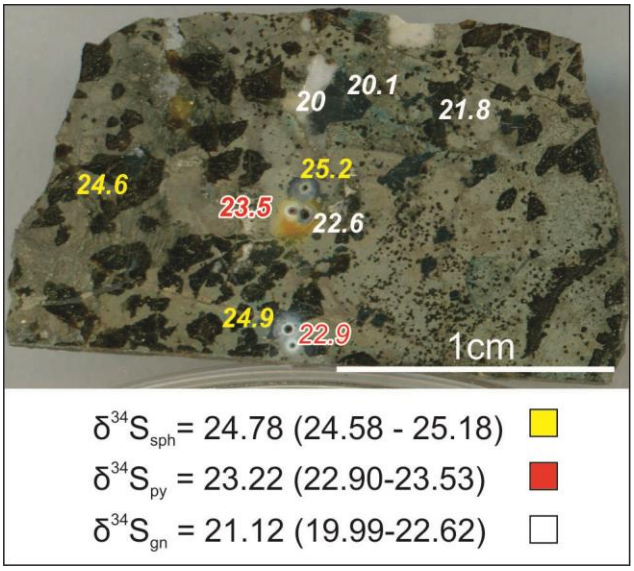

Figure 5. Photograph of sample PC93-23-249.7, an example of stratabound replacement sulphides from the Prairie Creek mine site, showing results of laser-assisted, in situ sulphur isotope analyses (colour coded as follows: yellow - sphalerite; red - pyrite; and white - galena), with sample averages and ranges for each mineral.

Stratabound Replacement Sulphides (SRS)

Sample **PC93-23-249.7** (Figure 5) of SRS shows idiomorphic sphalerite grains (ca. 20%) imbedded within fine-grained pyrite aggregate (ca. 50%). Several grains of galena (ca. 5%) and ca. 1% remnant dolostone (now coarse white spar calcite) and 3% chert are randomly distributed in this mottled dolostone member (OSw3-2) of the Whittaker Formation. Galena appears to have crystallized last, infilling remaining space. The relative isotopic compositions of pyrite and sphalerite are reversed from those expected for equilibrium, i.e. per mil fractionations between pyrite and sphalerite are negative (Appendix 2). This signifies isotopic disequilibrium, in contrast to the apparent textural equilibrium between the two minerals. Sphalerite evidently replaced pyrite without reaching isotopic equilibrium with its host. Similarly, the average pyrite-galena per mil fractionation (3.47‰) suggests an unreasonable average temperature of 317°C, likely due to the somewhat later crystallization of galena. Similarly, the per mil fractionation (0.91‰) between adjacent pyrite and galena grains (23.5 and

22.6‰, respectively) indicates a marked state of disequilibrium (T = 826°C, based on Kajiwara and Krouse, 1971). Yet, the similarity of compositions (20.1 and 20.0‰) measured in the same grain of galena (Figure 5) suggests that the other values of $\delta^{34}S$ noted elsewhere in the same sample (20.0 to 22.6‰) are likely valid. In situ measurements of separate grains of sphalerite and galena yield an average per mil fractionation of 3.66‰, consistent with a 'geologically reasonable' formation temperature of 220°C (Appendix 2).

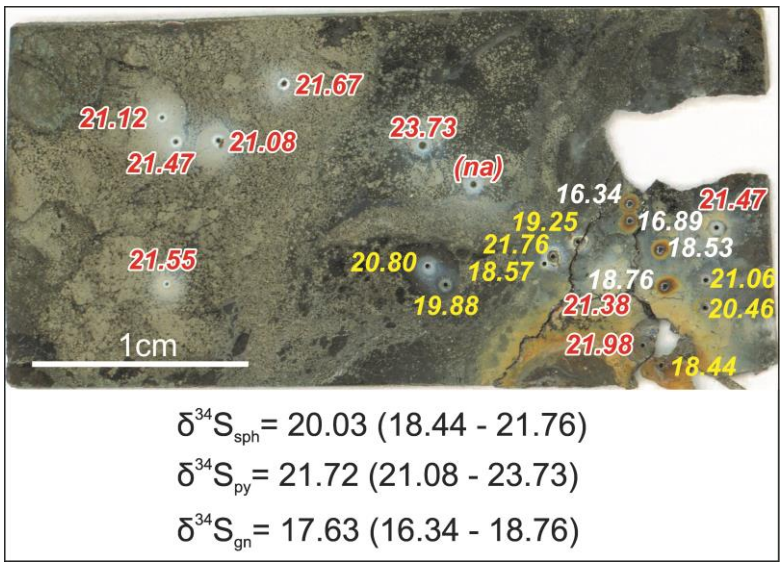

Figure 6. Photograph of sample PC92-19-289.5, an example of stratabound replacement sulphides from the Prairie Creek mine site, showing results of laser-assisted, in situ sulphur isotope analyses (color coded as in Figure 5), with sample averages and ranges for each mineral. In contrast to the relatively homogeneous isotopic composition of pyrite across the sample, galena and sphalerite are more diverse (see text for discussion).

Sample **PC92-19-289.5** (Figure 6) of SRS in OSw3-3 (Whittaker Formation) illustrates the textural diversity of pyrite, dominated by very fine-grained pyrite that has seemingly amalgamated to ill-defined areas of coarser, recrystallized pyrite. For the most part, the pyrite is relatively homogeneous in grain to grain sulphur isotope composition (21.1-22.0‰, with one anomalous result of 23.7‰; Figure 6). In contrast, sphalerite is more variable in $\delta^{34}S$ (18.6 to 21.1) on the mm-scale. Galena sulphur isotope compositions comprise two distinct groups (16.3-16.9‰ and 18.5-18.8‰) suggesting 'steps' or rapid gradations in isotopic composition across the sample. The sphalerite-galena temperature of 210°C represents an average of a range of 138 to 416°C. Figure 6 illustrates the difficulty in selecting which data points to associate for purpose of geothermometry; an average is perhaps the prudent approach in this case. The pyrite-galena fractionation suggesting a temperature of 239°C (Appendix 2) may seem reasonable on the surface, but the fractionation of 1.72 and estimated temperature of 148°C for pyrite-sphalerite call into question the results for pyrite-galena, and suggest that the similarity of pyrite-galena and sphalerite-galena temperatures is a matter of coincidence rather than fact. From a textural

perspective, sphalerite and galena appear in this sample (and others) to replace pyrite. In this case, attainment of isotopic equilibrium requires a multi-step process: dissolution, mixing, and precipitation. In addition, sphalerite replaced host dolostone, and sparry dolomite often occurs at the interface between dolostone and sphalerite during the mineralization process. We suggest that the sphalerite-galena temperature of 210°C is a reasonable estimate.

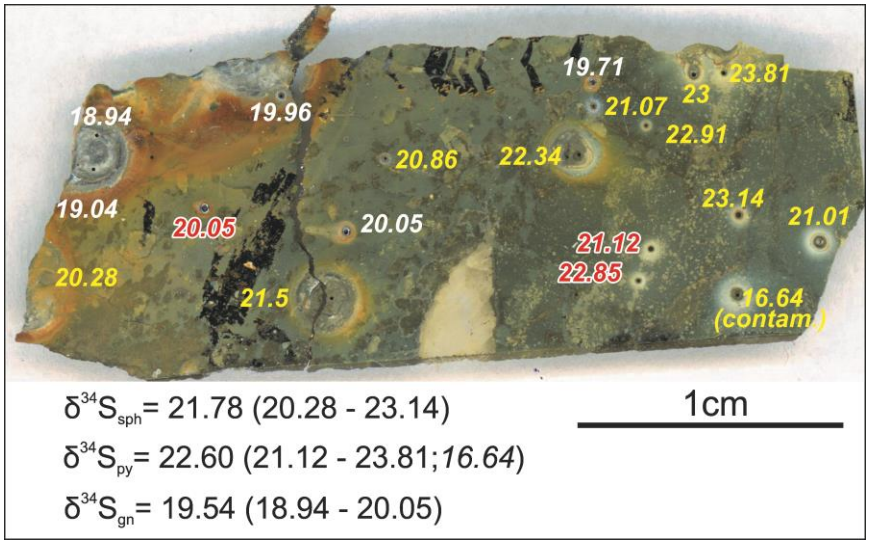

Figure 7. Photograph of sample PC94-64-207.6, an example of stratabound replacement sulphides from Zone 6, south of the Prairie Creek mine site (see Figure 2). Results for in situ analyses for sphalerite (yellow) and pyrite (red) suggest the presence of an isotopically enriched zone in the right hand half of the sample (see discussion in text).

Sample **PC94-64-207.6** (Figure 7) is representative of SRS in SD4 located in Zone 6, south of the Prairie Creek minesite (see Figure 2) in the upper spar unit, OSw3-6, of the Whittaker Formation. In situ analyses suggest compositional zoning on the millimetre-scale, with a band of higher $\delta^{34}S$ values found for sphalerite and pyrite in the right half of the sample, from the right of the carbonate filled vug. Per mil fractionations between bulk average compositions for pyrite, sphalerite and galena (Appendix 2) suggest broadly similar temperatures of 228°C (pyrite-sphalerite), 316°C (pyrite-galena) and 258°C (sphalerite-galena), excluding disequilibrium data. The individual pairing of data points does not always lead to a similar outcome in temperature, as the 'ne' (non-equilibrium) designation in Appendix 2 indicates. In the upper, central portion of the sample, however, nearest neighbour analyses of galena (19.7‰), and pyrite (22.3 and 22.9‰) yield temperatures of 281°C and 226°C; although pairing with the pyrite value of 21.1‰ (closest to the analyzed galena grain) yields an unrealistic temperature of 482°C. Thus, the fine-scale (µm to mm) inhomogeneity of sulphur isotope compositions in this sample, complicates the estimation of formation temperatures.

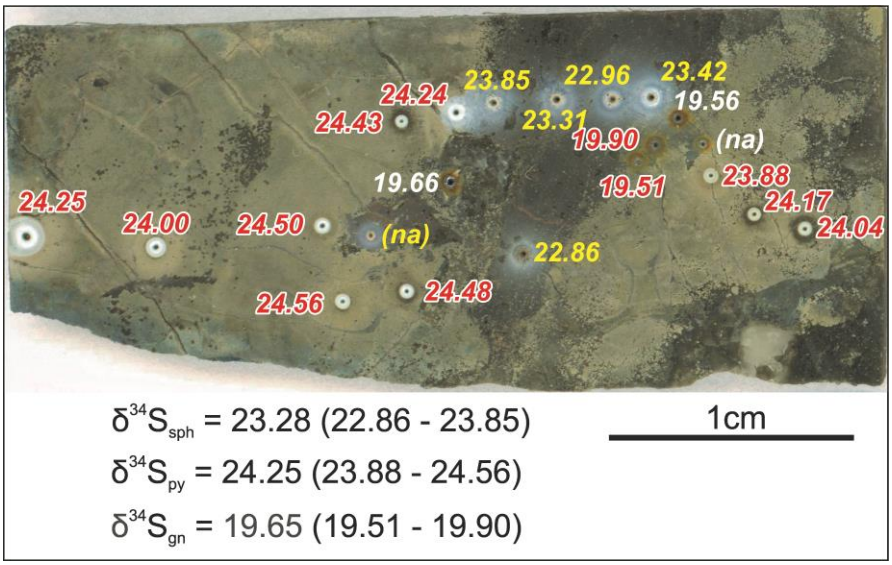

Figure 8. Photograph of sample PC93-25-251.9, an example of well-mineralized stratabound replacement sulphides in the OSw3-2 member of the Whittaker Formation (see Figure 2), from the outer margin of main sulphide body (see Figure 3). Results and locations of laser-assisted, in situ sulphur isotope analyses (colour code and abbreviations as in Figure 5) are shown, as well as sample averages and ranges for each mineral. Pyrite appears (ca. 60%) to form masses amalgamated from very-fine grained pyrite, consistent with its isotopic homogeneity across the sample. Sphalerite appears to increase in $\delta^{34}S$ as pyrite is approached, consistent with the replacement of pyrite by sphalerite (and, possibly later, galena). In addition to pyrite, the massive sulphide in this interval contains ca. 25% sph, 15% gal, 15% chert, 2% calcite, 2% quartz, and 2% white/gray dolomite.

Sample **PC93-25-251.9** (Figure 8) of SRS is from near the margin of the SD1 massive sulphide lens in OSw3-2 at the mine site (see Fig. 3). This sample represents a well-mineralized interval with 25% sphalerite and 15% galena, with accessory chert (15%), calcite (2%), quartz (2%), and white/gray dolomite (2%). Coarse sparry calcite (void fillings, or fragments?) is completely surrounded by galena. The homogeneous, nearly massive pyrite texture is matched by marked isotopic homogeneity (relative to some other samples), with a total apparent variation of ca. 1.0‰. Per mil fractionations between bulk average compositions for pyrite, sphalerite and galena (Appendix 2) suggest broadly similar temperatures of 282°C (pyrite-sphalerite), 216°C (pyrite-galena) and 164°C (sphalerite-galena). As with some other samples, the sphalerite-galena temperature can be the lowest of the three. In this case, its association with the outer limits of the sulphide body (see Figure 3) may have some significance.

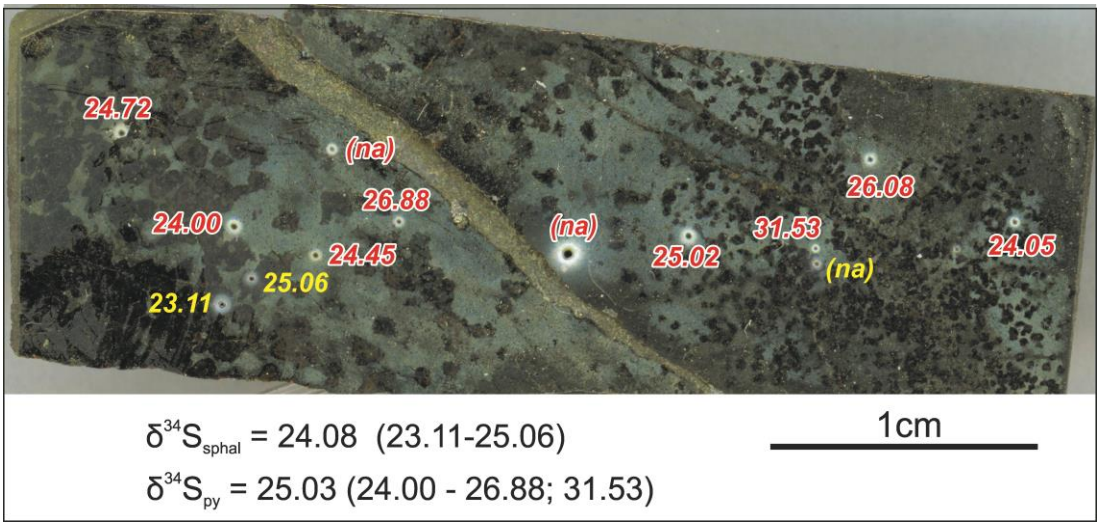

Figure 9. Photograph of sample PC01-130-313.5, an example of stratabound replacement sulphides from near the central region of the main sulphide lens SD1, Prairie Creek mine site (see Figure 3). Results and locations of laser-assisted, in situ sulphur isotope analyses (colour code and abbreviations as in Figure 5) are shown, as well as sample averages and ranges for each mineral. A pyrite matrix supports idiomorphic sphalerite; $\delta^{34}S$ of pyrite appears to increase from left to right, in concert with a decrease in grain size in sphalerite. The pyrite is quite homogeneous in isotopic composition, whereas isotopic variation in sphalerite may reflect replacement of pyrite by sphalerite (see discussion in text; value of 31.5 is anomalous and not considered).

Sample **PC01-130-313.5** (Figure 9) is from the SRS replacing the mottled dolostone member of the upper Whittaker Formation (OSw3-2). The sample shows idiomorphic pinkish sphalerite of variable size (size decreases left to right) enclosed within matrix pyrite. Minor galena and calcite fill remaining space in parts of the sample (not shown, nor analyzed). Sulphur isotope data for pyrite imply a slight enrichment in ^{34}S in the right half of the specimen. Only two analyses of sphalerite are available; the two per mil difference is marked considering their close proximity. Per mil fractionations between bulk average compositions for pyrite and sphalerite (Appendix 2) suggest a temperature of 165°C. This is lower than in other samples.

Mississippi Valley-type (MVT) Sulphides

Sample **PC94-75-204.5** (Figure 10) is from the MVT "Zebra showing" in the Root River Formation. It consists of cavities that are filled by sparry dolomite and are rimmed by pyrite. Marked sulphur isotope variation characterizes the pyrite in this sample, grading from 14.7 to 17.1‰ as the vug-filling sparry dolomite is approached. Since an increase in $\delta^{34}S$, from 14.7‰ in the core to 15.9‰ at the rim can also be documented in one grain, we surmise that the 14.7 to 17.1‰ variation represents an increase in $\delta^{34}S$ in time, and may signify the 'reservoir effect' of a smaller 'pool' of sulphur (i.e. more nearly closed system) than evident for the formation of the SRS.

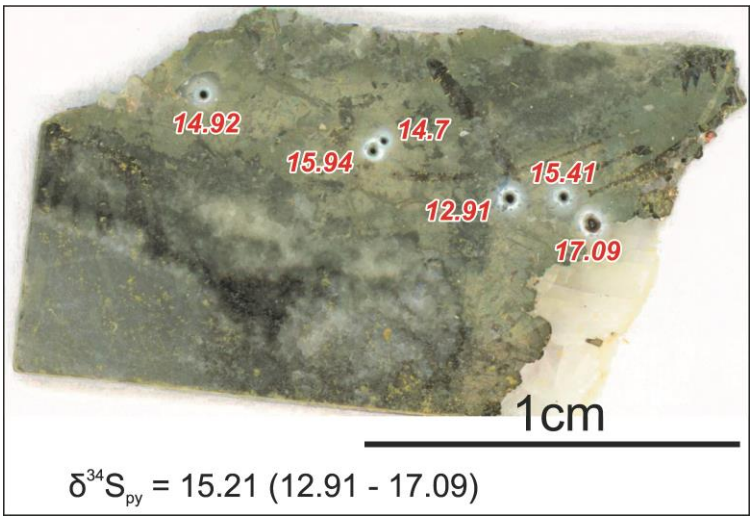

Figure 10. Photograph of sample PC94-75-204.5, an example of MVT-style sulphide mineralization from the Root River Formation. Marked sulphur isotope variation (see discussion in text) is consistent with a limited sulphur source (reservoir effect), or multiple sources of sulphur during formation (see text for discussion). The markedly lower sulphur isotope composition of pyrite in this sample relative to other, non-MVT style occurrences in the Prairie Creek district suggests a distinct origin.

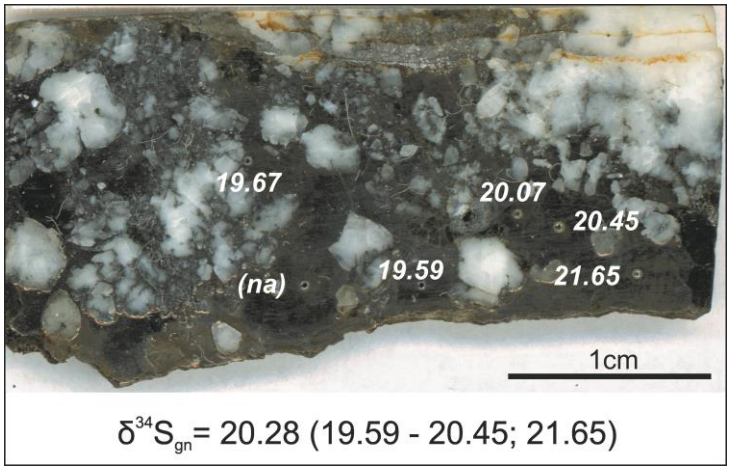

Figure 11. Photograph of sample PC95-125-760, an example of vein-style sulphide occurrence north of the Prairie Creek mine site (see Figure 2). The brecciated texture and stylolite-like contacts between some quartz grains suggests episodic vein filling and fault movement, followed by final annealing of groundmass galena. The sulphur isotope composition of galena suggests a gradient of increasing $\delta^{34}S$, left to right.

Quartz-carbonate-sulphide veins

Sample **PC95-125-760** (Figure 11) is from a quartz-carbonate-sulphide vein cross-cutting the Road River Formation north of the Prairie Creek mine site (see Figure 2A). It contains quartz, galena, occasional sphalerite, tetrahedrite-tennantite, and fragments (and/or void fillings) of calcite. The sample appears to have been brecciated, with quartz clasts 'suspended' in annealed galena matrix. Note the stylolite-like contacts between some quartz grains. In situ analyses of

galena appear to document a sulphur isotope gradient in $\delta^{34}S$, increasing from left to right. The orientation and global significance is not clear from this sample alone, but might be anticipated if vein-filling occurred over more than one episode, perhaps involving multiple fault movements and vein brecciation.

Discussion/Models

The juxtaposition of subsurface SRS lenses with the occasional outcropping of quartz-carbonate-sulphide veins and MVT occurrences in the Prairie Creek district, NT, prompted this study. The objective was to understand the origins and interrelationships, if any, of these three styles of base-metal sulphide occurrences with the hope of deriving useful criteria or guides for exploration. The fine-grained and texturally complex nature of the sulphide-bearing specimens called for the application of laser-assisted, micro-analysis to determine the sulphur isotope compositions of the essential minerals.

The principal questions addressed in this study included: 1) to what extent are the SRS, vein-, and MVT-style sulphide occurrences related? 2) What attributes of the mineralization processes (e.g. temperature) are related to sulphide occurrence and/or metal grade? 3) Are there any diagnostic, or helpful, isotopic characteristics that would be of use in mineral exploration (e.g. suggestive of sulphide deposition controls)? 4) Is it possible to discern the paleo-hydrology of the mineralizing fluids? As with any high-resolution investigation, some questions were answered, and new questions were generated.

Three Styles of Mineralization: Related or Not?

The occurrence of base metal sulphides as MVT, SRS, and quartz-carbonate-sulphide veins, in the same or similar host rocks of the Prairie Creek district begs the question as to their relationship. Are the products of these three 'styles' of mineralization genetically related, directly or indirectly, or not? Although addressed previously by Paradis (2007), who considered the vein and SRS unrelated, we re-examine the possible relationships in the light of this study.

The histogram plot of strontium isotope ratios ($^{87}Sr/^{86}Sr$) shown in Figure 12A illustrates the similarity between the compositions of the host dolostone and the quartz-carbonate-sulphide veins and SRS lenses. Carbonates analyzed from the sulphide occurrences represent unreplaced dolostone and/or recrystallized carbonate, now in the form of dolomite and calcite (sometimes referred to as 'hydrothermal carbonate'). The latter have the highest $^{87}Sr/^{86}Sr$ ratios in the Prairie Creek district (see Appendix 1; Paradis, 2007). A caveat, however, in the Sr isotope data is the unknown extent to which radioactive decay in clastic sedimentary components in the carbonate rocks may have modified the apparent initial $^{87}Sr/^{86}Sr$ ratios. This caveat, notwithstanding, the correspondence in isotope ratios of host dolostone and carbonate gangue associated with sulphides suggests control by the host lithology of the strontium isotope ratio balance

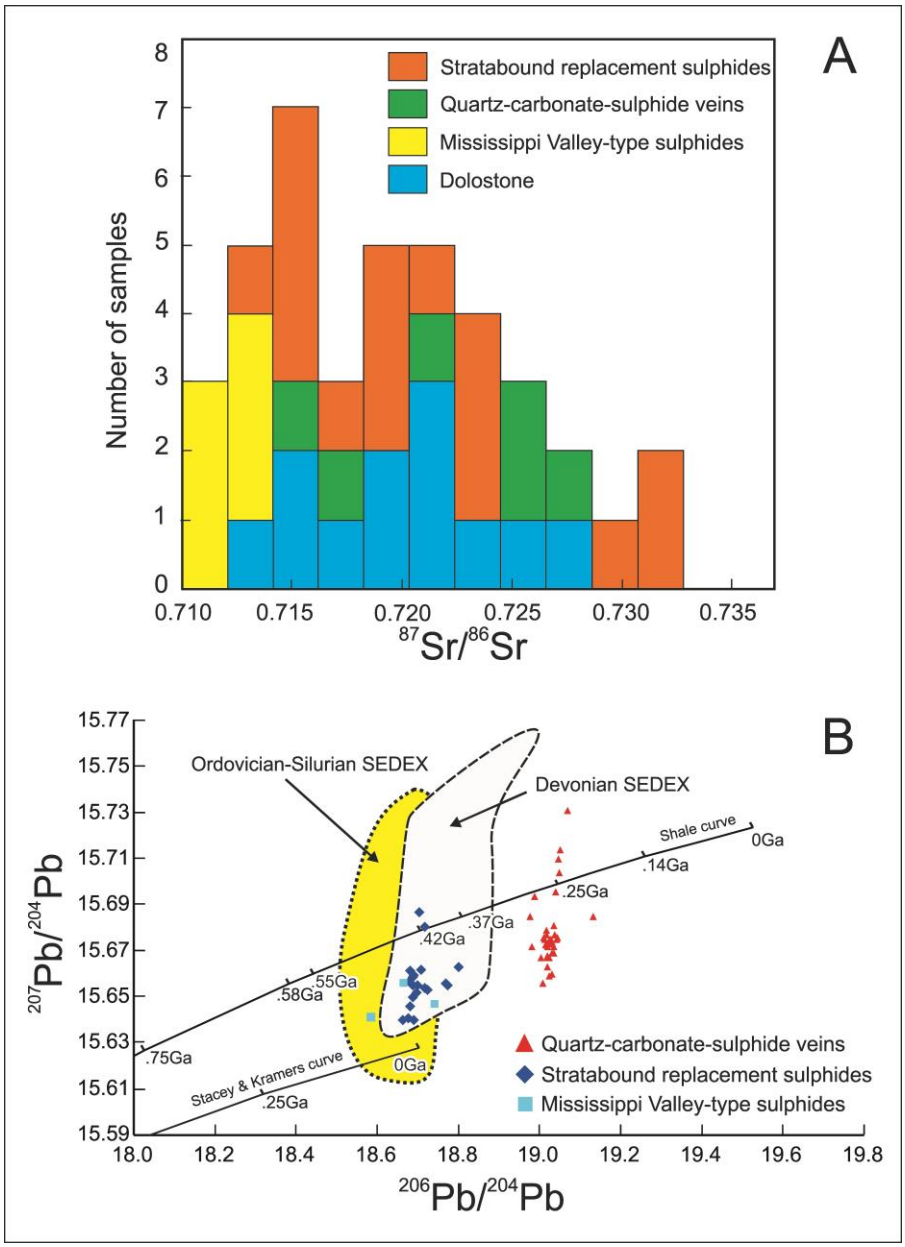

Figure 12A. Composite histogram of strontium isotope ratios measured on (primarily) carbonates from host dolostone and from stratabound, vein-type and MVT sulphide accumulations (data from Paradis, 2007, and references therein). The dolostone results represent those from the Upper Whittaker Formation, host to the vein and stratabound sulphides, whereas the MVT sulphides are hosted in the Root River Formation. The overlap in $^{78}Sr/^{86}Sr$ values indicates that the host-rocks control the strontium isotope abundances in the mineralized rocks. B. Plot of lead isotope ratios of Prairie Creek MVT, stratabound, and vein-style sulphide accumulations (Paradis, 2007). Whereas the stratabound and MVT types are of the same age, lead within the veins is consistent with a younger, perhaps Permian age, although the precise age is unknown. The "shale curve" is after Godwin and Sinclair (1982); the Stacey and Kramers terrestrial lead evolution curve is after Stacey and Kramers (1975).

during the mineralization process. Indeed, the MVT samples shown in Figure 12A are hosted within the Root River Formation, the latter of which yielded a low $^{87}Sr/^{86}Sr$ value of 0.7093 (see Figure 13C and p. 27 in Paradis, 2007), whereas vein- and stratabound sulphide samples hosted within the more radiogenic Upper Whittaker Formation yield higher values. Insofar as strontium isotopes are concerned as a tracer of fluid origins, the host rocks have, in each case, dominated the end result, masking any other possible source of strontium. In this respect, the veins and SRS may be said to share a common link. By virtue of different host rocks, the MVT sulphides do not share the same link.

In contrast to strontium isotopes, lead isotope ratios clearly distinguish the massive quartz-carbonate-sulphides from the SRS. In Figure 12B, the lead isotope ratios of sulphide minerals in vein occurrences plot on a trend suggesting a much later origin (e.g. Permian/Triassic transition) than the Silurian-Devonian origin implied for MVT and SRS. A distinct age is consistent with the observed relationship of the veins crosscutting the SRS lenses. The incorporation of 'younger' lead is a product, therefore, of later vein formation. In addition, the occurrence of tetrahedrite-tennantite as a few percent in the veins appears to be an additional, distinctive mineralogical characteristic. When found in SRS lenses, tetrahedrite-tennantite occurs only in trace amounts. Viewed in terms of lead isotope data only, the veins and SRS accumulations are not of the same age and not directly genetically related. In other words, the veins were not conduits for the hydrothermal fluids that formed the SRS lenses or the MVT sulphide occurrences. However, the tracer implications of the lead isotope data strictly apply to the lead (in galena) within the vein system. The possibility of similar sulphur and metal sources remains open.

Documentation of sulphur isotope compositions of the vein-, SRS- and MVT-style mineralization may contribute to understanding the genesis and possible relationships of the various sulphide occurrences. Previous sulphur isotope studies in the Prairie Creek district include those of Fraser (1996) and Paradis (2007), who analyzed samples of all three styles of mineralization. Comparison of the data acquired in this study and that acquired by Paradis (2007) and Fraser (1996) is necessary. However, the contrast in methods and analytical scales between the present study, using in situ laser-assisted fluorination producing single 130 µm reaction pits, and the averaging effects of mineral concentrates analyzed by oxidation to SO_2 (Fraser, 1996; Paradis, 2007) requires some interpretation/discussion when addressing isotopic characteristics and variations on larger scales.

Comparison of the sulphur isotope compositions of pyrite, sphalerite, and galena in the three styles of sulphide occurrences in the Prairie Creek district (Figure 13) indicates a variable degree of correspondence between the styles of sulphide occurrences, and between in situ measurements and bulk analyses of mineral concentrates. Although there are fewer measurements of 'bulk mineral concentrates' (Figure 13) compared to in situ measurements, there appears to be

a general agreement of both sets of data for pyrite, sphalerite and galena. With regard to pyrite and sphalerite from veins, however, there appears to be little agreement in $\delta^{34}S$ with values for SRS mineralization, although the number of measurements of veins is few. For galena (Figure 13C), good agreement exists between results for veins and SRS mineralization, whether measured on mineral concentrates or by in situ analysis.

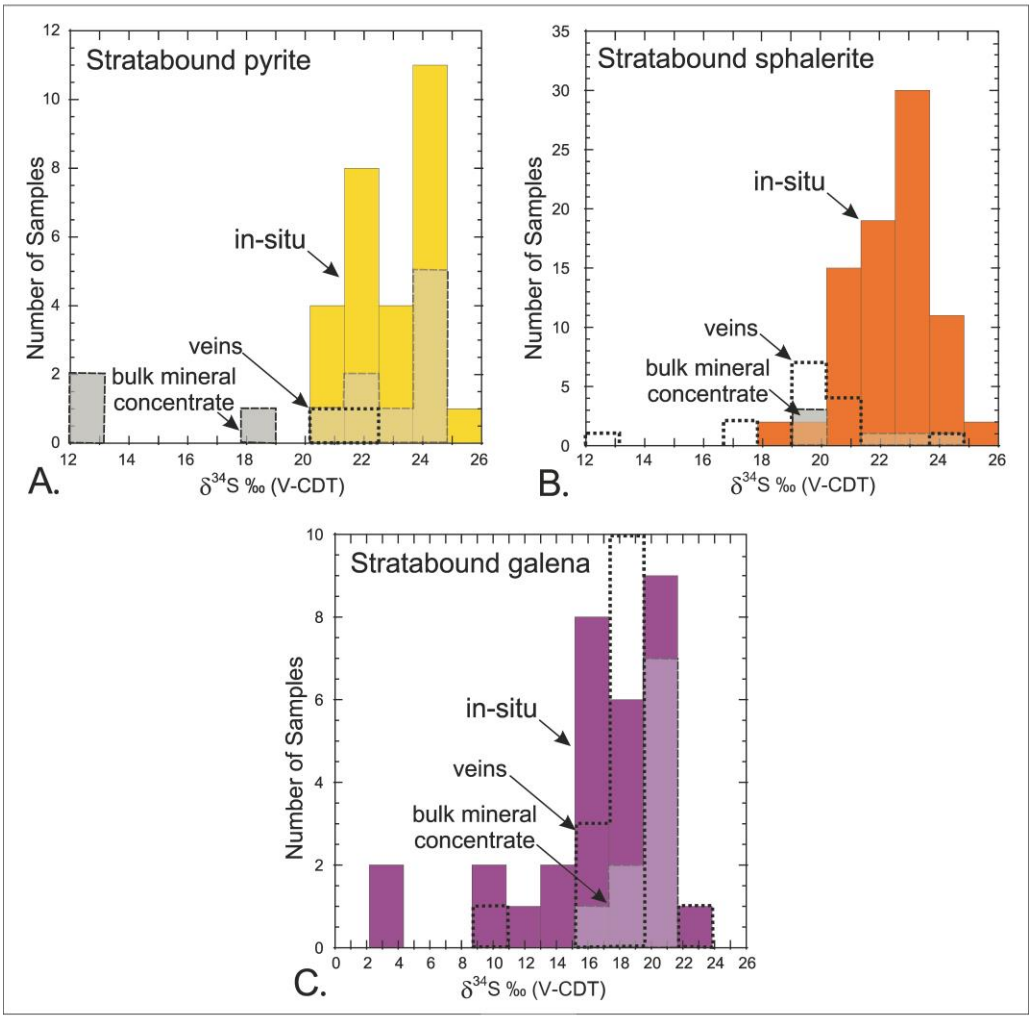

Figure 13. Composite histograms for sulphur isotope compositions of sulphide minerals from stratabound replacement sulphide lenses in the Prairie Creek district measured by in situ methods (this study), compared to results on mineral concentrates from vein and stratabound occurrences (Paradis, 2007).

Sphalerite is of particular interest inasmuch as the per mil fractionation between it and reduced hydrothermal sulphur is sufficiently small over the likely temperature range of formation of the SRS, MVT, and, perhaps, vein occurrences (e.g. Ohmoto and Rye, 1979), that sphalerite can form a proxy for the sulphur isotope composition of the mineralizing fluids (in this case, ca. 23‰). The correspondence between the $\delta^{34}S$ values of sphalerite from the SRS lenses and

from the veins determined by in situ measurement and bulk mineral concentrates (Figure 13B) is close, but not exact. Modes of distributions of $\delta^{34}S$ values from the veins and SRS mineral concentrates (see Figure 13B) are ca. 3‰ lighter than the mode for the in situ measurements. This might raise the question of possible analytical issues as an explanation, considering the very small analytical area (ca. 130 μm) of the in situ samples (e.g. complications raised by the opaque surface of the sample, possibility of nearest-neighbour interactions, etc.), were it not for the similarity of ranges of $\delta^{34}S$ for the mineral concentrate data and in situ measurements (i.e. there is not a consistent 'off set' to consider). Moreover, the number of analyses of mineral concentrates from the veins and SRS is few in comparison to the in situ measurements.

Galena in samples of SRS is 'late' in the crystallization sequence. The histogram of sulphur isotope compositions shows the closest correspondence between the SRS (both bulk mineral concentrate and in situ analyses) and the veins. The contrast between the vein-SRS agreement on galena and disagreement involving pyrite and sphalerite is striking. Viewed solely from the perspective of galena, the veins and SRS lenses appear to be closely related in terms of their sulphur sources. It raises that question as to whether this agreement indicates some sort of communication between vein-forming fluids and the SRS lenses.

Despite the relative age differences of the SRS and vein sulphide occurrences, and ignoring the specific exceptions noted above, the general similarity of the sulphur isotope data illustrated in Figure 13A-C suggests a similar sulphur source. There are two possible scenarios by which this may be satisfied. Firstly, we may hypothesize that later, vein-forming fluids remobilized sulphides from SRS lenses in the sedimentary section. In support of this possibility, we note the spatial association of veins and stratabound lenses, the galena sulphur isotope systematics, perhaps the contrast in tetrahedrite-tennantite abundance noted previously, and the likelihood that sulphur isotope disequilibrium between earlier formed sulphides could have resulted from limited interaction with vein-forming fluids. Alternatively, the similarity in sulphur source may be explained by extraction of (S-bearing) pore fluids or dissolution of marine sulphate from similar aged rocks during vein and SRS formation.

Considering reduced sea water sulphate as a potential sulphur source for the SRS lenses (Paradis, 2007), we note that the mean sulphur isotope composition of marine sulphate changed markedly from the Silurian-Devonian (ca. 20-25‰) to the Permian (ca. 13‰), decreasing about 10‰ (Kampschulte and Strauss, 2004). Despite whatever transfer mechanism might be envisioned (e.g. expulsed pore fluids, dissolution evaporitic sulphate, etc), the vein-contained sulphur could not have been derived from reduced Permian sea water sulphate (ca. 13‰). The sulphur isotope similarity between pyrite from SRS and from veins is striking: Paradis (2007) reported mean values of 19.52‰ (σ = 6.14) and 21.39‰ (σ = 0.42), respectively. Again, this similarity suggests a similar source (or isotopic composition) of sulphur for both veins and SRS. Reduced (Silurian-Devonian)

sea water sulphate (ca. 20-25‰; from pore fluid, or dissolution of sulphate minerals) is a permissible source for both. This scenario is perhaps broadly similar to that involving a “deeper, crustal source of sulphur” (see Paradis, 2007), but only if it satisfies the age constraint noted above.

The occurrence of nodular chert throughout the sedimentary host-rock section (see Appendix 2, Paradis, 2007) raises the question of “distance to source” with regard to sulphur, and bears on a topic not addressed in the current study: the causes of sulphide precipitation and whether more than one fluid was involved. The nodular texture of chert is commonly thought to derive from the replacement of sulphate minerals (directly) or by replacement of carbonates that are, themselves, replacements of earlier-formed sulphates (gypsum/anhydrite; e.g. Maliva and Siever, 1989; Henchiri and Slim-S’himi, 2006; Warren, 2006). The replacement process is thought to be early and may involve bacterial sulphate reduction. Transport of released sulphur into the basin, perhaps via saline fluids, would provide a source of appropriate age (and isotopic composition) sulphur (sulphide and/or sulphate). The very abundance of chert nodules might also suggest a source of sulphate for dissolution, subsequent to diagenesis.

The MVT occurrences in the Prairie Creek district (see Figure 2) have similar Pb isotope ratios for galena as found for the SRS mineralization (see Figure 12B) and are, therefore, of generally similar age (Paradis, 2007). The sulphur isotope compositions of the MVT sulphides, however, have markedly lower $\delta^{34}S$ values than either the SRS or the vein occurrences, and indicate a distinct sulphur source. Mean $\delta^{34}S$ values for MVT pyrite, galena and sphalerite reported by Paradis (2007) are 13.79‰, 13.06‰, and 13.61‰, respectively. These sulphides are clearly not in mutual isotopic equilibrium, but some 6‰ lower than in stratabound occurrences. This is likely due, in part, to sequential precipitation and/or recrystallization at different times and at different temperatures, probably from a more local source of sulphur than that which mineralized the Upper Whittaker Formation, forming SRS lenses. The isotopic gradients expressed by pyrite in PC94-75-204.5 (Figure 10), both from core (14.7‰) to rim (15.9‰) in one grain, and in the whole sample, from 12.9 to 17.1‰ indicate a changing sulphur isotope composition of the hydrothermal fluids during pyrite precipitation. This may have occurred by fluid (sulphur source) mixing, or, alternatively, and perhaps more likely in our view, a reservoir effect whereby the sulphur isotope composition of the hydrothermal fluid changed in response to sulphide precipitation. The latter scenario could be the consequence of a local sulphur source suggested above.

In reference to the SRS and quartz-carbonate-sulphide veins, the Pb and S isotope data indicate that the MVT occurrences appear to be genetically unrelated. The MVT occurrences formed about the same time as the SRS lenses, but from a different, local and limited source of sulphur. Local, host rock control of the Sr isotope compositions, in support of the above interpretation, was noted earlier.

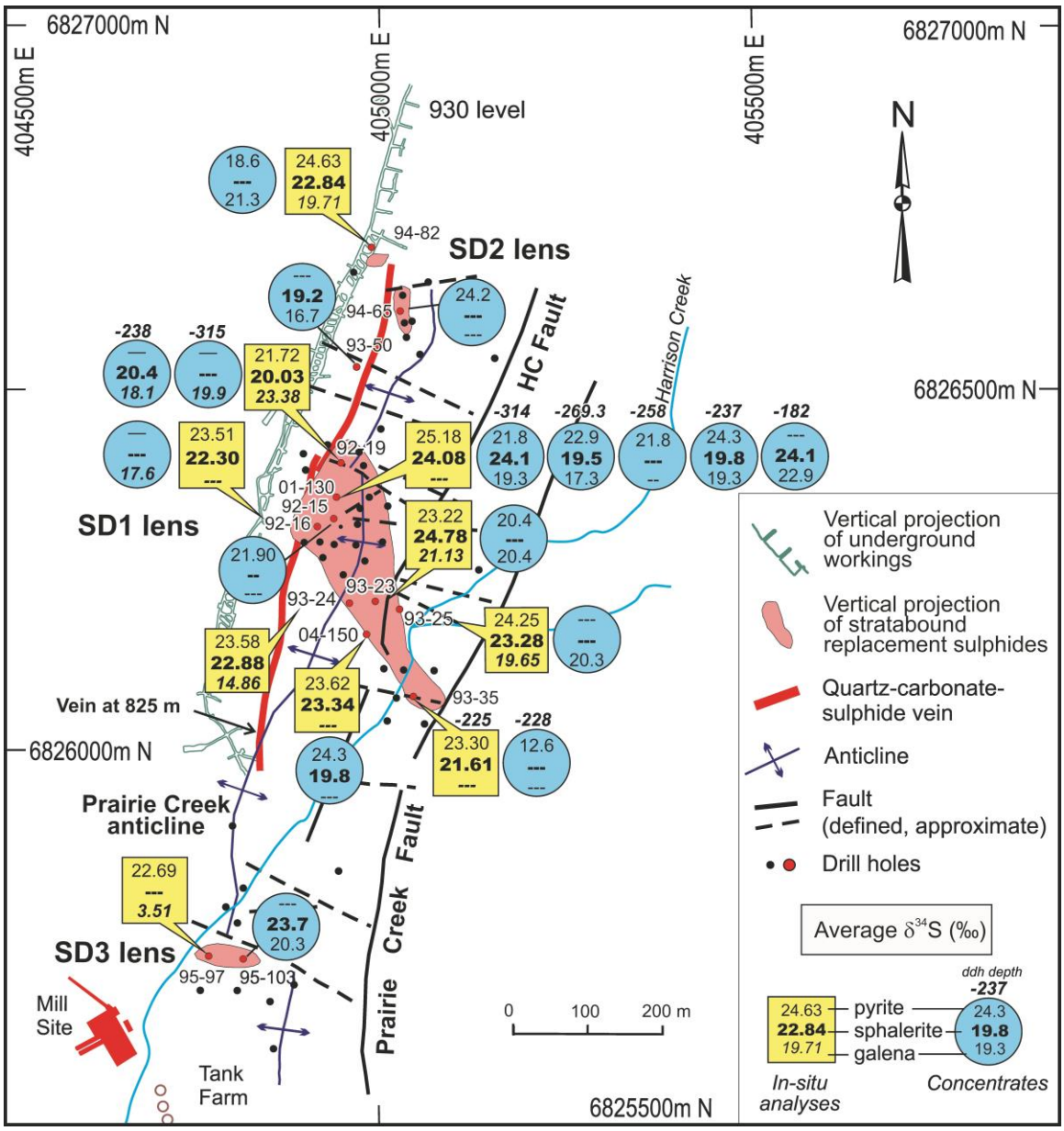

Figure 14. Map of the Prairie Creek mine area showing a projection of the stratabound replacement sulphide lenses, and the quartz-carbonate-sulphide veins, with $\delta^{34}S$ values for sphalerite, pyrite and galena from indicated sample sites. Data reported in yellow fields represents averages of in situ measurements in each samples (this study), whereas data plotted in blue fields are whole-rock analyses reported by Paradis (2007). For the latter, the depth intercepts of the core samples are noted (in meters). Little can be said regarding isotopic variation with depth, except for comparison of sphalerite from drill core 01-130 near the central axis of the projected ore body (Figure 14): the central portion of the stratabound massive sulphide body seems to be isotopically lighter than the upper and lower portions. In contrast, the margins of the stratabound sulphide lens SD1 seem to be isotopically heavier than the margins. Further investigation is needed to resolve these discrepancies.

Sulphur Isotope Variations within the Prairie Creek Mine Area

Average values of $\delta^{34}S$ for pyrite, sphalerite, and galena in samples of SRS were plotted in Figure 14, comparing data from whole-rock samples reported by Paradis (2007) and in situ measurements from this study, with the hope of elucidating general fluid pathways of the replacement process. A comparison using sample averages for in situ data provides a better basis when examining possible trends. Data from Paradis (2007) occasionally represent more than one sample per drillhole, permitting an assessment of vertical variation in $\delta^{34}S$ (the depth intercept of the sample in metres is shown with the isotopic compositions). In several cases, variations of several per mil occur within a few meters. More striking, however, is the occasional discordance in $\delta^{34}S$ between sample averages for in situ data and for whole-rock measurements. The discordance is most striking for pyrite (and galena in one anomalous sample; 95-97A, SD3 lens), and less so for sphalerite. The reason for these discrepancies is unclear at present. Therefore, we rely primarily on the in situ data set.

Sphalerite appears to be isotopically heaviest along the central axis of the projected outline of SD1 lens at the Prairie Creek mine site (Figure 14), between drillholes (DDH) 01-130 and 93-23. This could be used to infer that fluids flowed longest in this region, perhaps marking this as near an up-flow zone, since sphalerite, precipitating from a fluid of nearly constant sulphur isotope composition, increases in $\delta^{34}S$ with decreasing temperature (e.g. see Ohmoto and Rye, 1979). However, sulphur isotope gradients that might exist to map the flow paths of hydrothermal fluids are far from clear at this point, despite the present density of data. This suggests either a rather diffuse hydrothermal flow pattern, or that the replacement process occurred in such a way that simple flow paths were obscured by solution/redeposition occurring throughout a zone, guided by ever-changing, irregular porosity rather than by the progress of a simple replacement front. In this way, the small scale isotopic inhomogeneity documented in several samples may have resulted from the nature of fluid/rock interaction during replacement.

Thermal Variations and Possible Flow Directions in Stratabound Replacement Sulphides (SRS)

Paleotemperatures were estimated from the calibration equations of Kajiwara and Krouse (1971) based on per mil sulphur isotope fractionations between pyrite, sphalerite and galena. Although other calibrations are available in the literature, those of Kajiwara and Krouse provide a consistent basis for comparison. In addition, the calculated temperatures are reasonable, since the sphalerite-galena geothermometer was confirmed by close agreement with Rye (1974) who compared isotopic temperatures with fluid inclusion filling temperatures.

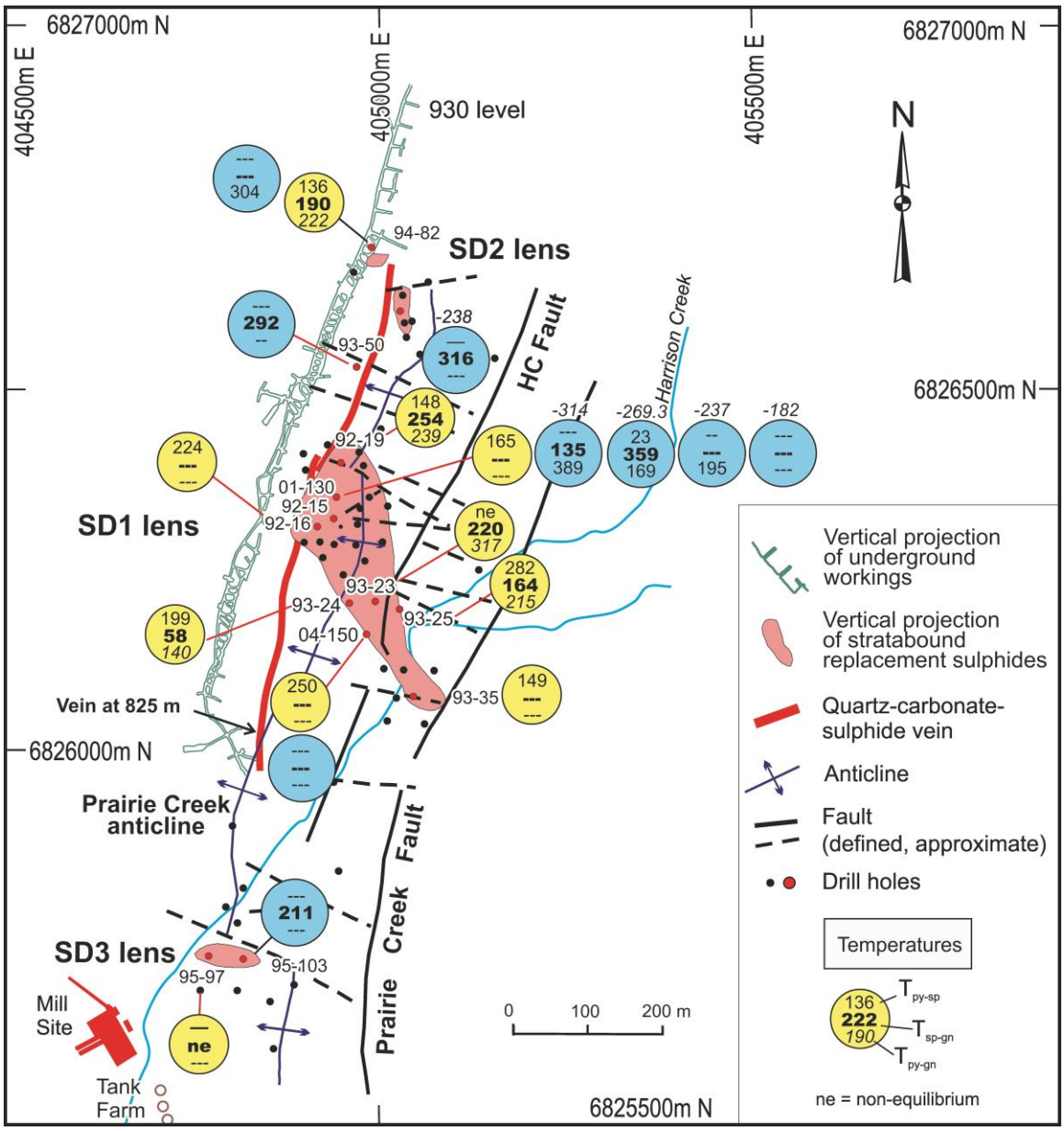

Figure 15. Map of the Prairie Creek mine area showing a projection of the stratabound sulphide lenses, and the quartz-carbonate-sulphide veins. Estimated temperatures (°C) based on average per mil S-isotope fractionations between sphalerite, pyrite and galena are shown based on in situ measurements (this study; yellow background) and whole-rock analyses (Paradis, 2007; blue background). In many cases, the calculated temperatures clearly indicate disequilibrium, which is denoted by dashed lines (also used where insufficient data, or a missing mineral, prevented an estimate of temperature). The intercept depths to each of several samples from the same drill core are shown as in Figure 14. The sphalerite-galena pair appears to provide the best temperature estimates, having formed together; these are ca. 165-255ºC. Additional temperature estimates will be available upon completion of this project, although disequilibrium is common (see text).

From inspection of the isotopic temperatures plotted in Figure 15, it appears that disequilibrium is the rule rather than the exception, most especially where pyrite is involved. Both the textural relationships and the relative degree of isotopic homogeneity compared to sphalerite present in, for example, PC92-19-289.5 (Figure 6) and PC93-25-251.9 (Figure 8), suggest that pyrite and sphalerite are not co-genetic. Rather, sphalerite appears to have partially replaced pyrite in some cases. In these situations, isotopic disequilibrium is not surprising, but characteristic of a protracted mineralizing process. Any remaining sulphate in the host rocks (i.e. unreplaced by chert) might have further promoted the disequilibrium. In other situations, such as those involving pyrite and galena, galena may have approached equilibrium with pyrite through the solution/redeposition processes of replacement. A number of pyrite-galena temperatures near 200°C (Figure 15) may have achieved their similarity in this way, even though pyrite and galena did not co-precipitate.

Based on sphalerite-galena temperatures, the central axial region of the projected outline of SD1, between DDH 92-19 and 93-23, seems to record higher temperatures than elsewhere. The data currently available suggest that sphalerite-galena pairs record a thermal gradient decreasing to the southeast, along the length of the projection of SD1 (Figure 15), away from the quartz-carbonate-sulphide vein. It may be that this massive vein follows, or is near to the ancestral position of a fault zone that had acted as a hydrothermal conduit for sulphide mineralization. Of course, the vein cross-cuts the folded sedimentary section (Figure 2) and cannot correspond, itself, to a paleo-hydrothermal channel. But, was the strike of the vein system influenced by an ancestral hydrothermal conduit? The locations of smaller sulphide bodies (e.g. SD2 and SD3) would be consistent with such a hypothesis.

Formation of the Stratabound Replacement Sulphide (SRS) Lenses

The precise age of formation of the SRS lenses is not known. The Pb isotope data provide a general answer consistent with a broadly similar age to the enclosing rocks, but permits an origin that could be somewhat later. The true age bears on the possible relationship of the mineralized Prairie Creek vein to the SRS lenses. The location of the main, SRS lens (SD1) near the high point of a doubly-plunging anticline in the Prairie Creek district, raises the possibility that replacement may have occurred early, during folding. Figure 2B illustrates the fact that the Prairie Creek vein is not axial planar with the present fold. But, was it initially? Was the Prairie Creek vein rotated somewhat during folding?

Sulphur isotope data discussed previously are compatible with a common source of sulphur, whereas Pb isotope data (see Figure 12) require a later phase of hydrothermal activity for the veins. The physical association of vein and SRS might suggest that the vein developed from what was originally a hydrothermal conduit. Textural evidence (Paradis, 2007) suggests multiple filling/deformation events in the Prairie Creek vein's history. Perhaps this is a record which

developed during and subsequent to folding and early replacement of the mottled dolostone (Upper Whittaker Formation).

Implications for Exploration

We infer that up-welling, metalliferous hydrothermal fluids reacted with, and replaced, the stratigraphically lowest susceptible (carbonate-bearing) member of the Whittaker Formation. Any residual sulphate in the Whittaker Formation may have contributed a local source of sulphur. With this in mind, and the results of this study, the following implications are:

- An exploration focus on the same or similar (stratigraphically low) units to the OSw3-2 (mottled dolostone, Whittaker Formation) in the subsurface may prove useful.

- The location of replacement sulphide bodies (in plan view) may have been controlled by ancestral faults. The fact that such sulphide bodies seem to align with the principal anticlinal axis in the Prairie Creek district suggests that sulphide occurrences may have been at least partially responsible for, or otherwise involved with, fold axis localization. If so, similar structural settings may be provide for fruitful exploration.

- The quartz-carbonate-sulphide veins, which formed much later than the SRS lenses, seem to have filled post-ore faults that may have been either localized by ancestral, mineralization-related structural weaknesses, or related to folding of the sedimentary host rocks.

- The sulphur isotope compositions of the vein and are consistent with a similar sulphur source either by remobilization of earlier-formed, SRS, or by derivation of sulphur (pore fluid, or dissolution of marine sulphate) from the same or similar rocks, albeit at different times. Pb isotope ratios are consistent with latter scenario. Thus, the geographic occurrence and abundance of sulphides in veins may offer a clue to the subsurface mineral potential of the area.

- The limited data available on the “MVT-style” of sulphide occurrence indicates that they cannot be easily related to the SRS or vein sulphide occurrences, and may be of limited interest for exploration.

Future Work

Analyses from twenty-four samples currently in progress (extracted but requiring mass spectrometry) will geographically broaden the data base presently available, and facilitate a more comprehensive interpretation. Completion of the study as originally planned was made difficult by interruptions to analytical facilities and scheduling. The in situ and grain analyses in progress will allow a more comprehensive investigation of possible compositional variations in the Prairie Creek district, and address the difficult question of possible thermal

gradients. Knowledge of thermal gradients in the SRS lenses, if they can be documented, may help to decipher fluid flow and vectors of use to exploration.

Acknowledgements

We are grateful to Canadian Zinc Corporation for granting access to the property and allowing us to sample drill core. All personnel of Canadian Zinc Corporation and, specifically, Alan Taylor and Kerry Cupit provided invaluable geological information that is much appreciated. André Pellerin and Thi Hao Bui (McGill University) were very helpful in providing an introduction to gas chromatographic (GC) purification of SF_6 gas samples prior to mass spectrometry. In addition, André Pellerin provided helpful suggestions during the addition, design and installation of a gas chromatograph and related vacuum plumbing on MILES (LSI lab, Ottawa), and during the design and installation (BET) of a micro-sample inlet on the mass spectrometer in the Department of Earth and Planetary Sciences, McGill University to measure the small samples from this study. The review comments of W.D. Goodfellow and A. Rukhlov are gratefully acknowledged.

References

AMC Mining Consultants (Canada), 2012, Prairie Creek Property, Northwest Territories, Canada. Technical Report for Canadian Zinc Corporation, unpublished report, rev. July 23, 2014, 209 p. [http://www.canadianzinc.com/projects/prairie-creek/resources].

Asprey, L. B., 1976, The preparation of very pure fluorine gas: Journal Fluorine Chemistry, v. 7, p. 359-361.

Beaudoin G, Taylor, B.E., 1994, High-precision and spatial-resolution sulfur isotope analysis using MILES laser microprobe. Geochimica et Cosmochimica Acta 58: 5055-5063.

Beaudoin, G., and Therrien, P., 2004, The web stable isotope fractionation calculator, *in* Handbook of stable isotope analytical techniques, Volume-I. De Groot, P.A., ed., Analytical Techniques 1: Elsevier, p. 1045-1047.

Earls, G., 1995, A review of the Prairie Creek deposit, NT, Canada: Internal Report, San Andreas Resources Corporation, 36 p.

Fraser, S.C.,1996, Geology and geochemistry of the Prairie Creek Zn, Pb, Ag deposits, Southern Mackenzie Mountains, Northwest Territories: Unpublished M.Sc. thesis, University of Alberta, Edmonton, Alberta, 146 p.

Godwin, C.I. and Sinclair, A.J.,1982, Average lead isotope growth curves for shale-hosted zinc lead deposits, Canadian Cordillera; Economic Geology, v. 77, p. 675-690.

Goodfellow, W.D., and Lydon, J.W., 2007, Sedimentary exhalative (SEDEX) deposits, *in* Goodfellow, W.D., ed., Mineral deposits of Canada: A synthesis of major deposit types, district metallogeny, the evolution of geological provinces, and exploration methods: Geological Association of Canada, Mineral Deposits Division, Special Publication no. 5, p. 163-183.

Henchiri, M., and Slim-S'himi, N., 2006, Silicification of sulphate evaporites and their carbonate replacements in Eocene marine sediments, Tunisia: two diagenetic trends: Sedimentology, v. 53, p. 1135-1159.

Kajiwara, Y., and Krouse, H.R., 1971, Sulphur isotope partitioning in metallic sulphide systems: Canadian Journal of Earth Science v. 8, p. 1397-1408.

Kampschulte, A., and Strauss, H., 2004, The sulphur isotopic evolution of Phanerozoic seawater based on the analysis of structurally substituted sulfate in carbonates: Chemical Geology, v. 302, p. 255-286.

Maliva, R. G., and Siever, R., 1989, Nodular chert formation in carbonate rocks: Journal of Geology, v. 97, p. 421-433.

Morrow, D.W., and Cook, D.G., 1987, The Prairie Creek Embayment and Lower Paleozoic strata of the southern Mackenzie Mountains: Geological Survey of Canada, Memoir 412, 195 p.

Ohmoto, H., and Rye, R. O., 1979, Isotopes of sulphur and carbon, *in* Barnes, H. L. ed., Geochemistry of Hydrothermal deposit: John Wiley & Sons, p. 509-567.

Paradis, S., 2007, Isotope geochemistry of the Prairie Creek carbonate-hosted zinc-lead-silver deposit, southern Mackenzie Mountains, Northwest Territories, *in* Wright, D. F., Lemkow, D., and Harris, J., ed., Mineral and energy potential of the proposed expansion to the Nahanni National Park Reserve, North Cordillera, Northwest Territories: Geological Survey of Canada, Open File 5344, p. 1-46.

Rye, R.O., 1974, A comparison of sphalerite-galena sulphur isotope temperatures with filling temperatures of fluid inclusions: Economic Geology, v. 69, pp. 26-32.

Stacey, J.S. and Kramers, J.D., 1975, Approximation of terrestrial lead isotope evolution by a two-stage model; Earth and Planetary Science Letters, v. 26, p. 207-221.

Taylor, B. E., 2004a, Biogenic and thermogenic sulfate reduction in the Sullivan Pb-Zn-Ag deposit, British Columbia (Canada): Evidence from micro-isotopic analysis of carbonate and sulphide in bedded ores: Chemical Geology, v. 204, p. 215–236.

Taylor, B. E., 2004b, Fluorination methods in stable isotope analysis, *in*, de Groot, P.A., ed., Handbook of Stable Isotope Analytical Techniques 1: Elsevier, p. 400 – 472.

Taylor, B.E., and Beaudoin, G., 1993, MILES laser microprobe, Part 1: System description: Geological Survey of Canada, Current Research, Part D, Paper 1993-ID, p. 191-198.

Taylor, B.E., Paradis, S., Falck, H., and Wing, B., in preparation, Sulphur isotope studies Pb-Zn mineralization, Prairie Creek, southern Mackenzie Mountains, Northwest Territories.

Warren, J.K., 2006, Evaporites: Sediments, resources and hydrocarbons: Springer-Verlag, Berlin. 1035 p.

Appendix 1. Sulphur isotope compositions of individual sulphide grains and/or analytical traverses within individual sulphide grains.

Extraction / Lab Number	General Sample Description	Field Spl No.	Mineral	$\delta^{33}S_{VCDT}$	$\delta^{34}S_{VCDT}$	$\delta^{36}S_{VCDT}$	$\Delta^{33}S_{VCDT}$	$\Delta^{36}S_{VCDT}$	δ^{34}Spy	δ^{34}Ssphal	δ^{34}Sgn
MIV-104-2/LSI-05-09-1	SRS in mottled dolo unit of OSw3-2.	PC01-130-313.5	py	14.4	26.9	1551.42	0.65	1537.66	*26.8***		
MIV-104-3/LSI-05-09-1	Bands of fg py in agg of fg pinkish sphal	PC01-130-313.5	py	12.9	24.5	793.89	0.37	781.37	24.5		
MIV-104-5/LSI-05-09-1	and fg py; gn and cc fill remaining	PC01-130-313.5	py	12.5	24.0	490.25	0.17	477.96	24.0		
MIV-104-6/LSI-05-09-1	spaces.	PC01-130-313.5	py	12.7	24.7	908.09	0.09	895.43	24.7		
MIV-103-10/LSI-05-09-1		PC01-130-313.5	py	13.6	26.1	6761.72	0.28	6748.37	*26.1***		
MIV-103-11/LSI-05-09-1		PC01-130-313.5	py	19.0	31.5	14219.51	2.86	14203.39	*31.5***		
MIV-103-9/LSI-05-09-1		PC01-130-313.5	py	14.3	24.0	1336.14	1.99	1323.83	24.0		
MIV-105-10/LSI-05-09-1		PC01-130-313.5	sphal	13.4	25.1	888.20	0.57	875.38		25.06	
MIV-105-9/LSI-05-09-1		PC01-130-313.5	sphal	11.9	23.1	246.30	0.04	234.46		23.11	
								AVG.	**24.3**	**24.08**	
MIV-107-10/LSI-05-09-2	SRS in OSw3-2.	PC04-150-238.6	py	13.8	24.3	170.65	1.36	158.22	24.3		
MIV-107-11/LSI-05-09-2	Sulphides comprise agg of fg py + sphal	PC04-150-238.6	py	12.9	23.8	213.12	0.66	200.93	23.8		
MIV-107-12/LSI-05-09-2	replacing the cherty dol.	PC04-150-238.6	py	12.0	23.4	215.36	-0.04	203.36	23.4		
MIV-107-2/LSI-05-09-2	Gn and cc fill remaining spaces.	PC04-150-238.6	py	13.6	22.8	347.27	1.99	335.61	22.8		
MIV-107-3/LSI-05-09-2		PC04-150-238.6	py	19.0	25.6	4261.45	5.93	4248.35	*25.6***		
MIV-107-9/LSI-05-09-2		PC04-150-238.6	py	11.9	23.8	371.59	-0.31	359.40	23.8		
MIV-107-4/LSI-05-09-2		PC04-150-238.6	sphal	12.7	24.8	2421.36	-0.03	2408.66	24.8	24.79	
MIV-107-6/LSI-05-09-2		PC04-150-238.6	sphal	14.7	23.6	3050.80	2.63	3038.73		23.58	
MIV-107-7/LSI-05-09-2		PC04-150-238.6	sphal	12.3	24.1	2189.70	-0.04	2177.37		24.08	
MIV-107-8/LSI-05-09-2		PC04-150-238.6	sphal	12.3	23.5	211.09	0.27	199.08		23.46	
MIV-108-1/LSI-05-09-2		PC04-150-238.6	sphal	11.8	24.7	1880.82	-0.88	1868.16		24.73	
MIV-108-2/LSI-05-09-2		PC04-150-238.6	sphal	11.2	22.0	328.18	-0.08	316.89		22.04	
MIV-108-3/LSI-05-09-2		PC04-150-238.6	sphal	12.4	22.3	249.08	0.99	237.67		22.27	
MIV-108-4/LSI-05-09-2		PC04-150-238.6	sphal	11.6	22.9	352.14	-0.11	340.39		22.94	
MIV-108-5/LSI-05-09-2		PC04-150-238.6	sphal	11.8	24.5	743.58	-0.68	731.06		24.45	
MIV-108-6/LSI-05-09-2		PC04-150-238.6	sphal	11.9	23.5	539.69	-0.10	527.66		23.47	
								AVG.	**23.8**	**23.58**	
MIV-104-11/LSI-05-09-3	SRS in OSw3-2.	PC92-16-310.6	py	10.9	21.3	182.70	0.01	171.78	21.3		
MIV-104-7/LSI-05-09-3	Layered sulp mix with chert nodules.	PC92-16-310.6	py	11.9	22.1	248.82	0.61	237.53	22.1		
MIV-104-8/LSI-05-09-3	Sulph are fg mix of spha, py, gn.	PC92-16-310.6	py	11.4	22.3	265.82	-0.02	254.39	22.3		
MIV-105-2/LSI-05-09-3		PC92-16-310.6	py	12.3	22.9	514.37	0.58	502.62	22.9		
MIV-105-5/LSI-05-09-3		PC92-16-310.6	py	12.0	21.0	2916.70	1.26	2905.92	21.0		
MIV-105-6/LSI-05-09-3		PC92-16-310.6	py	11.6	22.5	1723.66	0.09	1712.13	22.5		
MIV-103-12/LSI-05-09-3		PC92-16-310.6	py	13.0	25.0	2637.08	0.17	2624.28	25.0		
MIV-104-9/LSI-05-09-3		PC92-16-310.6	sphal	13.4	25.8	896.49	0.16	883.29		25.79	
MIV-105-1/LSI-05-09-3		PC92-16-310.6	sphal	12.5	22.7	386.65	0.91	375.03		22.67	
MIV-105-3/LSI-05-09-3		PC92-16-310.6	sphal	11.7	22.5	262.37	0.16	250.84		22.50	
MIV-105-7/LSI-05-09-3		PC92-16-310.6	sphal	11.6	22.7	1007.55	-0.06	995.92		22.71	
MIV-105-8/LSI-05-09-3		PC92-16-310.6	sphal	11.4	22.3	310.93	-0.01	299.49		22.34	
								AVG.	**22.5**	**23.20**	
MIV-123-7/LSI-05-09-04	SRS in OSw3-3.	PC92-19-289.5	py	12.1	23.7	75.26	-0.01	63.11	23.7		
MIV-123-8/LSI-05-09-04	Fg agg of py adjacent to crystalline dol	PC92-19-289.5	py	11.1	21.7	78.51	0.00	67.40	21.7		
MIV-123-9/LSI-05-09-04	and cg gn.	PC92-19-289.5	py	10.8	21.1	85.16	0.05	74.36	21.1		
MIV-123-10/LSI-05-09-04		PC92-19-289.5	py	10.8	21.1	101.67	0.00	90.85	21.1		
MIV-123-11/LSI-05-09-04		PC92-19-289.5	py	11.0	21.5	71.55	-0.01	60.55	21.5		
MIV-123-12/LSI-05-09-04		PC92-19-289.5	py	11.0	21.6	105.11	-0.03	94.07	21.6		

Appendix 1 continued.

Extraction / Lab Number	General Sample Description	Field Spl No.	Mineral	$\delta^{33}S_{VCDT}$	$\delta^{34}S_{VCDT}$	$\delta^{36}S_{VCDT}$	$\Delta^{33}S_{VCDT}$	$\Delta^{36}S_{VCDT}$	δ^{34}Spy	δ^{34}Ssphal	δ^{34}Sgn
MIV-122-4/LSI-05-09-04		PC92-19-289.5	py	11.3	22.0	186.27	0.05	175.02	22.0		
MIV-122-7/LSI-05-09-04		PC92-19-289.5	py	11.0	21.4	387.38	0.08	376.43	21.4		
MIV-122-8/LSI-05-09-04		PC92-19-289.5	py	11.4	21.5	401.00	0.42	390.00	21.5		
MIV-122-3/LSI-05-09-04		PC92-19-289.5	sphal	9.5	18.4	71.77	0.03	62.31		18.44	
MIV-122-5/LSI-05-09-04		PC92-19-289.5	sphal	9.9	19.2	287.89	0.05	382.69		19.25	
MIV-122-6/LSI-05-09-04		PC92-19-289.5	sphal	9.6	18.6	392.21	0.05	382.69		18.57	
MIV-122-9/LSI-05-09-04		PC92-19-289.5	sphal	10.9	21.1	289.03	0.10	278.24		21.06	
MIV-122-10/LSI-05-09-04		PC92-19-289.5	sphal	10.6	20.5	360.06	0.12	349.58		20.46	
MIV-123-3/LSI-05-09-04		PC92-19-289.5	sphal	11.1	21.8	67.82	-0.01	56.67		21.76	
MIV-123-4/LSI-05-09-04		PC92-19-289.5	sphal	10.8	20.8	108.48	0.19	97.82		20.80	
MIV-123-5/LSI-05-09-04		PC92-19-289.5	sphal	10.2	19.9	91.17	0.04	80.98		19.88	
MIV-122-11/LSI-05-09-04		PC92-19-289.5	gn	9.6	18.8	484.85	0.03	475.23			18.76
MIV-122-12/LSI-05-09-04		PC92-19-289.5	gn	9.5	18.5	255.39	0.00	245.89			18.53
MIV-123-1/LSI-05-09-04		PC92-19-289.5	gn	8.9	16.9	378.91	0.25	370.24			16.89
MIV-123-2/LSI-05-09-04		PC92-19-289.5	gn	8.6	16.3	201.22	0.17	192.84			16.34
								AVG.	**21.7**	**20.03**	**17.63**
MIV-120-4/LSI-05-09-05	SRS in OSw3-2.	PC93-25-251.9	py	12.4	24.0	724.67	0.07	712.36	24.0		
MIV-120-5/LSI-05-09-05	Fg agg of py with interstitial gn.	PC93-25-251.9	py	12.3	24.2	338.08	-0.07	325.71	24.2		
MIV-120-6/LSI-05-09-05	coarse sparry cc fills remaining spaces.	PC93-25-251.9	py	12.2	23.9	263.21	-0.06	250.99	23.9		
MIV-121-3/LSI-05-09-05	Composite content: 25% sphal, 15% gn,	PC93-25-251.9	py	12.4	24.2	643.71	0.01	631.30	24.2		
MIV-121-4/LSI-05-09-05	15% chert, 2% cc, 2% qz, and	PC93-25-251.9	py	12.6	24.4	1454.32	0.09	1441.82	24.4		
MIV-121-7/LSI-05-09-05	2% white/gray dol.	PC93-25-251.9	py	12.9	24.5	116.26	0.41	103.73	24.5		
MIV-121-8/LSI-05-09-05		PC93-25-251.9	py	12.7	24.6	104.32	0.12	91.75	24.6		
MIV-121-10/LSI-05-09-05		PC93-25-251.9	py	12.5	24.5	461.74	-0.05	449.19	24.5		
MIV-121-11/LSI-05-09-05		PC93-25-251.9	py	12.4	24.0	261.73	0.13	249.44	24.0		
MIV-121-12/LSI-05-09-05		PC93-25-251.9	py	12.4	24.3	128.12	-0.01	115.70	24.3		
MIV-120-11/LSI-05-09-05		PC93-25-251.9	sphal	12.0	23.4	123.37	0.01	111.38		23.42	
MIV-120-12/LSI-05-09-05		PC93-25-251.9	sphal	11.8	23.0	175.79	0.06	164.04		22.96	
MIV-121-1/LSI-05-09-05		PC93-25-251.9	sphal	12.1	23.3	1276.15	0.19	1264.21		23.31	
MIV-121--2/LSI-05-09-05		PC93-25-251.9	sphal	12.3	23.9	1715.26	0.07	1703.05		23.85	
MIV-121-6/LSI-05-09-05		PC93-25-251.9	sphal	12.2	22.9	5866.14	0.46	5854.43		22.86	
MIV-120-8/LSI-05-09-05		PC93-25-251.9	gn	10.0	19.5	372.79	0.02	362.79			19.51
MIV-120-9/LSI-05-09-05		PC93-25-251.9	gn	10.2	19.9	403.71	0.05	393.51			19.90
MIV-120-10/LSI-05-09-05		PC93-25-251.9	gn	10.1	19.6	224.45	0.04	214.42			19.56
MIV-121-5/LSI-05-09-05		PC93-25-251.9	gn	10.2	19.7	4247.37	0.09	4237.29			19.66
								AVG.	**24.3**	**23.28**	**19.65**
MIV-114-11/LSI-05-09-06	SRS in OSw3-2.	PC93-24-257.1	py	12.0	23.6	366.77	-0.07	354.65	23.6		
MIV-114-12/LSI-05-09-06	Diss fg py in cherty band, and sphal in	PC93-24-257.1	py	11.9	23.2	272.17	0.03	260.27	23.2		
MIV-115-6/LSI-05-09-06	siliceous dolo; veinlets of py criss-cut dolo.	PC93-24-257.1	py	11.8	23.3	109.21	-0.12	97.26	23.3		
MIV-116-1/LSI-05-09-06	Section resembles stringers.	PC93-24-257.1	py	11.9	23.5	207.88	-0.12	195.83	23.5		
MIV-116-10/LSI-05-09-06	Composite content: py (40%), sphal (10%),	PC93-24-257.1	py	12.2	23.7	657.86	0.09	645.75	23.7		
MIV-116-3/LSI-05-09-06	ga (3%), and 30% dark grey dol.	PC93-24-257.1	py	11.9	23.5	189.93	-0.12	177.89	23.5		
MIV-116-4/LSI-05-09-06		PC93-24-257.1	py	12.4	24.5	280.58	-0.16	268.03	24.5		
MIV-115-8/LSI-05-09-06		PC93-24-257.1	py	11.8	23.2	194.25	-0.06	182.36	23.2		
MIV-117-9/LSI-05-09-06		PC93-24-257.1	py	11.9	23.6	192.64	-0.14	180.56	23.6		
MIV-114-10/LSI-05-09-06		PC93-24-257.1	sphal	12.6	23.6	639.66	0.51	627.60		23.56	
MIV-114-8/LSI-05-09-06		PC93-24-257.1	sphal	17.2	22.6	840.50	5.64	828.93		22.57	

Appendix 1 continued.

Extraction / Lab Number	General Sample Description	Field Spl No.	Mineral	$\delta^{33}S_{VCDT}$	$\delta^{34}S_{VCDT}$	$\delta^{36}S_{VCDT}$	$\Delta^{33}S_{VCDT}$	$\Delta^{36}S_{VCDT}$	δ^{34}Spy	δ^{34}Ssphal	δ^{34}Sgn
MIV-114-9/LSI-05-09-06		PC93-24-257.1	sphal	12.3	23.3	557.32	0.32	545.37		23.33	
MIV-115-1/LSI-05-09-06		PC93-24-257.1	sphal	11.8	22.4	217.73	0.29	206.23		22.44	
MIV-115-10/LSI-05-09-06		PC93-24-257.1	sphal	12.6	24.8	104.18	-0.09	91.50		24.78	
MIV-115-2/LSI-05-09-0		PC93-24-257.1	sphal	12.1	22.5	206.15	0.62	194.63		22.49	
MIV-115-3/LSI-05-09-06		PC93-24-257.1	sphal	11.2	22.2	241.66	-0.11	230.30		22.16	
MIV-115-7/LSI-05-09-06		PC93-24-257.1	sphal	12.5	22.9	132.31	0.79	120.56		22.94	
MIV-115-9/LSI-05-09-06		PC93-24-257.1	sphal	12.3	24.0	153.56	-0.03	141.25		24.05	
MIV-116-11/LSI-05-09-06		PC93-24-257.1	sphal	11.1	22.5	471.62	-0.39	460.11		22.48	
MIV-116-12/LSI-05-09-06		PC93-24-257.1	sphal	12.1	23.9	221.05	-0.10	208.83		23.87	
MIV-116-2/LSI-05-09-06		PC93-24-257.1	sphal	11.6	23.0	224.34	-0.18	212.54		23.03	
MIV-116-5/LSI-05-09-06		PC93-24-257.1	sphal	12.0	23.5	161.41	-0.03	149.37		23.52	
MIV-116-6/LSI-05-09-06		PC93-24-257.1	sphal	10.7	20.8	276.45	0.08	265.79		20.80	
MIV-116-7/LSI-05-09-06		PC93-24-257.1	sphal	10.9	21.1	126.73	0.07	115.95		21.06	
MIV-117-2/LSI-05-09-06		PC93-24-257.1	sphal	13.3	23.9	230.47	1.06	218.24		23.89	
MIV-117-6/LSI-05-09-06		PC93-24-257.1	sphal	11.7	22.0	180.35	0.43	169.06		22.03	
MIV-117-7/LSI-05-09-06		PC93-24-257.1	sphal	12.3	22.6	109.54	0.72	97.94		22.65	
MIV-117-8/LSI-05-09-06		PC93-24-257.1	sphal	11.9	23.1	168.06	0.05	156.20		23.14	
MIV-115-11/LSI-05-09-06		PC93-24-257.1	gn	7.6	15.4	279.26	-0.29	271.38			15.36
MIV-115-12/LSI-05-09-06		PC93-24-257.1	gn	6.9	14.3	313.03	-0.38	305.71			14.26
MIV-115-4/LSI-05-09-06		PC93-24-257.1	gn	6.4	10.8	235.63	0.87	230.10			10.76
MIV-115-5/LSI-05-09-06		PC93-24-257.1	gn	8.3	12.6	357.20	1.89	350.74			12.57
MIV-116-8,-9/LSI-05-09-06		PC93-24-257.1	gn	8.7	18.0	588.49	-0.56	579.28			17.96
MIV-117-1/LSI-05-09-06		PC93-24-257.1	gn	7.7	15.6	312.40	-0.28	304.38			15.63
MIV-117-3/LSI-05-09-06		PC93-24-257.1	gn	30.5	20.4	13680.36	20.08	13669.92			20.38
MIV-117-4/LSI-05-09-06		PC93-24-257.1	gn	8.4	16.0	919.62	0.15	911.39			16.03
MIV-117-5/LSI-05-09-06		PC93-24-257.1	gn	6.0	10.8	341.55	0.46	336.00			10.80
								AVG.	**23.6**	**22.88**	**14.86**
MIV-110-2/LSI-05-09-7	SRS in OSw3-2.	PC93-35-224.8	py	19.0	36.3	5252.11	0.48	5233.60	*36.3***		
MIV-110-3/LSI-05-09-7	Section of fg mas py and pink to yellow	PC93-35-224.8	py	12.1	24.3	1055.28	-0.31	1042.84	*24.3***		
MIV-110-4/LSI-05-09-7	sphal cutting cherty dol. Pink sphal is mixed	PC93-35-224.8	py	11.6	23.0	713.44	-0.20	701.67	23.0		
MIV-110-5/LSI-05-09-7	with py; yellowish spha cut the agg of py.	PC93-35-224.8	py	11.5	23.3	735.72	-0.48	723.77	23.3		
MIV-110-8/LSI-05-09-7		PC93-35-224.8	py	11.7	23.5	672.12	-0.29	660.08	23.5		
MIV-110-9/LSI-05-09-7		PC93-35-224.8	py	11.4	22.4	627.79	0.00	616.34	22.4		
MIV-110-10/LSI-05-09-7		PC93-35-224.8	sphal	12.0	22.0	195.22	0.77	183.96		21.98	
MIV-110-11/LSI-05-09-7		PC93-35-224.8	sphal	11.9	23.0	865.14	0.14	853.37		22.99	
MIV-110-12/LSI-05-09-7		PC93-35-224.8	sphal	10.8	21.3	426.06	-0.16	415.12		21.34	
MIV-110-6/LSI-05-09-7		PC93-35-224.8	sphal	10.4	20.6	266.06	-0.14	255.51		20.60	
MIV-110-7/LSI-05-09-7		PC93-35-224.8	sphal	11.2	21.7	287.21	0.10	276.10		21.68	
MIV-111-1/LSI-05-09-7		PC93-35-224.8	sphal	10.9	21.2	440.84	0.08	429.97		21.20	
MIV-111-2/LSI-05-09-7		PC93-35-224.8	sphal	10.8	21.4	388.75	-0.14	377.81		21.36	
MIV-111-3/LSI-05-09-7		PC93-35-224.8	sphal	11.1	21.8	178.30	-0.06	167.15		21.76	
								AVG.	**23.0**	**21.61**	
MIV-126-1/LSI-05-09-08	SRS in OSw3-4.	PC93-41-246.7	py	11.2	21.8	132.12	0.00	120.96	21.8		
MIV-126-3/LSI-05-09-08	Sulphide zones connected by fine ca 1 mm	PC93-41-246.7	py	10.4	20.4	181.41	-0.06	170.97	20.4		
MIV-126-6/LSI-05-09-08	mineralized qz-sphal-py-gn stringers.	PC93-41-246.7	py	11.8	23.3	439.49	-0.08	427.57	23.3		
MIV-127-9/LSI-05-09-08		PC93-41-246.7	py	11.9	23.6	389.04	-0.16	376.98	23.6		
MIV-125-9/LSI-05-09-08		PC93-41-246.7	sphal	12.3	23.9	127.05	0.09	114.83		23.86	

Appendix 1 continued.

Extraction / Lab Number	General Sample Description	Field Spl No.	Mineral	$\delta^{33}S_{VCDT}$	$\delta^{34}S_{VCDT}$	$\delta^{36}S_{VCDT}$	$\Delta^{33}S_{VCDT}$	$\Delta^{36}S_{VCDT}$	δ^{34}Spy	δ^{34}Ssphal	δ^{34}Sgn
MIV-125-10/LSI-05-09-08		PC93-41-246.7	sphal	11.4	22.4	120.65	-0.04	109.17		22.42	
MIV-126-12/LSI-05-09-08		PC93-41-246.7	sphal	9.0	17.6	123.17	0.01	114.17		*17.55***	
MIV-127-2/LSI-05-09-08		PC93-41-246.7	sphal	10.4	20.4	66.96	-0.08	56.52		20.37	
MIV-127-3/LSI-05-09-08		PC93-41-246.7	sphal	10.3	20.2	87.75	-0.01	77.40		20.18	
MIV-126-2/LSI-05-09-08		PC93-41-246.7	sphal	10.9	21.5	295.59	-0.08	284.59		21.47	
MIV-126-7/LSI-05-09-08		PC93-41-246.7	sphal	11.7	23.1	903.83	-0.17	892.00		23.11	
MIV-126-9/LSI-05-09-08		PC93-41-246.7	sphal	11.7	23.0	174.53	-0.06	162.75		23.01	
MIV-127-6/LSI-05-09-08		PC93-41-246.7	sphal	11.2	22.4	214.01	-0.21	202.55		22.36	
MIV-127-7/LSI-05-09-08		PC93-41-246.7	sphal	10.6	21.1	190.16	-0.15	179.36		21.07	
MIV-127-8/LSI-05-09-08		PC93-41-246.7	sphal	12.0	22.7	673.87	0.40	662.23		22.72	
MIV-127-10/LSI-05-09-08		PC93-41-246.7	sphal	12.3	24.2	283.29	-0.15	270.89		24.22	
MIV-127-11/LSI-05-09-08		PC93-41-246.7	sphal	11.5	22.5	125.33	0.01	113.79		22.53	
MIV-127-12/LSI-05-09-08		PC93-41-246.7	sphal	11.8	23.2	327.00	-0.07	315.14		23.16	
MIV-127-4/LSI-05-09-08		PC93-41-246.7	gn	7.9	15.8	149.66	-0.17	141.54			15.81
MIV-127-5/LSI-05-09-08		PC93-41-246.7	gn	7.6	15.2	225.71	-0.20	217.92			15.18
MIV-126-8/LSI-05-09-08		PC93-41-246.7	gn	7.3	14.6	332.23	-0.22	324.73			14.62
								AVG.	**22.2**	**22.34**	**15.21**
MIV-112-5/LSI-05-09-09	SRS in OSw3-6.	PC94-64-207.6	py	8.9	16.6	189.38	0.33	180.84	*16.6***		
MIV-112-6/LSI-05-09-09	Fg aggregates of py-sphal-gn.	PC94-64-207.6	py	11.6	22.9	191.62	-0.09	179.91	22.9		
MIV-112-7/LSI-05-09-09		PC94-64-207.6	py	10.8	21.1	210.63	-0.07	199.80	21.1		
MIV-112-8/LSI-05-09-09		PC94-64-207.6	py	12.4	23.8	210.80	0.16	198.60	23.8		
MIV-112-10/LSI-05-09-09		PC94-64-207.6	sphal	11.6	22.9	179.05	-0.12	167.31		22.91	
MIV-112-11/LSI-05-09-09		PC94-64-207.6	sphal	11.4	22.3	183.76	-0.03	172.32		22.34	
MIV-112-12/LSI-05-09-09		PC94-64-207.6	sphal	11.1	21.5	113.97	0.14	102.98		21.46	
MIV-112-3/LSI-05-09-09		PC94-64-207.6	sphal	11.0	21.0	223.98	0.22	213.22		21.01	
MIV-112-4/LSI-05-09-09		PC94-64-207.6	sphal	12.0	23.1	235.96	0.17	224.11		23.14	
MIV-112-9/LSI-05-09-09		PC94-64-207.6	sphal	11.9	23.0	146.79	0.16	135.01		23.00	
MIV-113-1/LSI-05-09-09		PC94-64-207.6	sphal	10.5	20.3	93.39	0.06	83.00		20.28	
MIV-113-4/LSI-05-09-09		PC94-64-207.6	sphal	10.6	20.9	116.61	-0.08	105.92		20.86	
MIV-113-8/LSI-05-09-09		PC94-64-207.6	sphal	10.6	21.1	144.25	-0.19	133.45		21.07	
MIV-113-2/LSI-05-09-09		PC94-64-207.6	gn	9.6	18.9	143.39	-0.10	133.67			18.94
MIV-113-3/LSI-05-09-09		PC94-64-207.6	gn	9.7	19.0	138.22	-0.10	128.46			19.04
MIV-113-5/LSI-05-09-09		PC94-64-207.6	gn	10.6	20.0	104.03	0.34	93.81			19.96
MIV-113-6/LSI-05-09-09		PC94-64-207.6	gn	10.2	20.1	130.86	-0.10	120.58			20.05
MIV-113-7/LSI-05-09-09		PC94-64-207.6	gn	10.0	19.7	135.64	-0.13	125.54			19.71
								AVG.	**22.6**	**21.78**	**19.54**
MIV-113-12/LSI-05-09-10	MVT sulph, Root River Fm.	PC94-75-204.5	py	7.6	14.9	114.47	-0.08	106.81	14.9		
MIV-114-1/LSI-05-09-10	Sample of sparry dol-filled vugs	PC94-75-204.5	py	7.4	14.7	143.38	-0.19	135.82	14.7		
MIV-114-1/LSI-05-09-10	rimmed by py.	PC94-75-204.5	py	7.4	14.7	143.38	-0.19	135.82	14.7		
MIV-114-2/LSI-05-09-10		PC94-75-204.5	py	8.0	15.9	156.82	-0.14	148.64	15.9		
MIV-114-3/LSI-05-09-10		PC94-75-204.5	py	6.6	12.9	140.46	-0.07	133.83	12.9		
MIV-114-4/LSI-05-09-10		PC94-75-204.5	py	7.7	15.4	261.57	-0.18	253.66	15.4		
MIV-114-5/LSI-05-09-10		PC94-75-204.5	py	8.7	17.1	325.15	-0.08	316.38	17.1		
								AVG.	**15.1**		
MIV-124-8/LSI-05-09-11	SRS in OSw3-4.	PC94-82-496.1	py	12.2	23.7	243.85	0.03	231.71	23.7		
MIV-124-10/LSI-05-09-11	Aggregate of fg py and sphal with	PC94-82-496.1	py	12.7	24.9	345.18	0.01	332.45	24.9		

Appendix 1 continued.

Extraction / Lab Number	General Sample Description	Field Spl No.	Mineral	$\delta^{33}S_{VCDT}$	$\delta^{34}S_{VCDT}$	$\delta^{36}S_{VCDT}$	$\Delta^{33}S_{VCDT}$	$\Delta^{36}S_{VCDT}$	δ^{34}Spy	δ^{34}Ssphal	δ^{34}Sgn
MIV-124-11/LSI-05-09-11	interstitial gn.	PC94-82-496.1	py	12.9	24.6	6528.93	0.31	6516.35	24.6		
MIV-124-12/LSI-05-09-11		PC94-82-496.1	py	12.7	24.8	1295.28	0.02	1282.59	24.8		
MIV-125-2/LSI-05-09-11		PC94-82-496.1	py	12.8	24.4	152.87	0.33	140.37	24.4		
MIV-125-3/LSI-05-09-11		PC94-82-496.1	py	12.9	25.2	106.73	0.05	93.83	25.2		
MIV-125-4/LSI-05-09-11		PC94-82-496.1	py	12.9	24.9	139.94	0.16	127.21	24.9		
MIV-124-9/LSI-05-09-11		PC94-82-496.1	sphal	11.7	22.8	124.19	-0.03	112.49		22.84	
MIV-124-4/LSI-05-09-11		PC94-82-496.1	gn	11.3	21.8	504.49	0.14	493.33			21.78
MIV-124-6/LSI-05-09-11		PC94-82-496.1	gn	9.9	19.3	242.76	0.05	232.88			19.27
MIV-124-7/LSI-05-09-11		PC94-82-496.1	gn	9.0	17.3	764.79	0.16	755.91			17.32
MIV-125-5/LSI-05-09-11		PC94-82-496.1	gn	10.9	20.5	380.46	0.40	369.97			20.45
								AVG.	**24.6**	**22.84**	**19.71**
MIV-118-7/LSI-05-09-12	SRS in OSw3-2.	PC95-97-79.1	py	11.7	22.9	312.65	-0.01	300.93	22.9		
MIV-118-8/LSI-05-09-12	Mas to semi-mas sulph comprised of	PC95-97-79.1	py	11.6	22.8	314.98	-0.05	303.32	22.8		
MIV-118-12/LSI-05-09-12	fg py (50%), reddish-brown sphal (35%)	PC95-97-79.1	py	10.5	20.0	131.75	0.26	121.49	20.0		
MIV-119-1/LSI-05-09-12	and gn; sphal partially replaced black chert	PC95-97-79.1	py	12.7	23.7	144.65	0.60	132.52	23.7		
MIV-119-06/LSI-05-09-12	nodules.	PC95-97-79.1	py	11.1	21.6	141.08			21.6		
MIV-119-07/LSI-05-09-12		PC95-97-79.1	py	12.1	23.6	109.28			23.6		
MIV-119-08/LSI-05-09-12		PC95-97-79.1	py	12.0	23.6	129.90			23.6		
MIV-119-11/LSI-05-09-12		PC95-97-79.1	gn	1.7	3.1	1025.89	0.09	1024.32			3.06
MIV-119-12/LSI-05-09-12		PC95-97-79.1	gn	2.4	4.0	12157.80	0.39	12155.76			3.96
								AVG.	**22.6**		**3.51**
MIV-111-10/LSI-05-09-13	Qz-Carb-Sulph vein in Road River Fm.	PC95-125-760	gn	10.0	19.6	427.42	-0.08	417.37			19.59
MIV-111-12/LSI-05-09-13	Qz-gn +/- sphal, tetra-tenn vein with late	PC95-125-760	gn	9.8	19.7	530.68	-0.26	520.60			19.67
MIV-111-6/LSI-05-09-13	cc blobs.	PC95-125-760	gn	11.1	21.6	3363.89	-0.04	3352.79			21.65
MIV-111-7/LSI-05-09-13		PC95-125-760	gn	10.8	20.4	763.49	0.32	753.01			20.45
MIV-111-8/LSI-05-09-13		PC95-125-760	gn	10.0	20.1	668.72	-0.25	658.43			20.07
								AVG.			**20.28**
MIV-108-10/LSI-05-09-14	SRS in OSw3-2.	PC93-23-249.7	py	11.9	23.5	263.41	-0.18	251.36	23.5		
MIV-108-11/LSI-05-09-14	Agg of fg py and cg sphal, and ga grains.	PC93-23-249.7	py	11.4	22.9	333.48	-0.35		22.9		
MIV-108-7/LSI-05-09-14	Composite section: Sphal 20%, Gn 5%,	PC93-23-249.7	sphal	12.5	24.6	348.50	-0.08	335.91		24.58	
MIV-108-9/LSI-05-09-14	50% Py, 1% white spar, approx 3% chert.	PC93-23-249.7	sphal	12.5	25.2	399.81	-0.35	386.92		25.18	
MIV-109-6/LSI-05-09-14		PC93-23-249.7	sphal	12.6	24.6	533.54	0.00	520.95		24.60	
MIV-108-12/LSI-05-09-14		PC93-23-249.7	gn	12.8	20.0	19.99	2.53				19.99
MIV-108-8/LSI-05-09-14		PC93-23-249.7	gn	11.5	22.6	196.59	-0.09	185.00			22.62
MIV-109-1/LSI-05-09-14		PC93-23-249.7	gn	10.4	20.1	500.55	0.04	490.23			20.14
MIV-109-4/LSI-05-09-14		PC93-23-249.7	gn	10.7	21.7	3150.17	-0.48	3139.03			21.75
								AVG.	**23.2**	**24.78**	**21.12**

Abbreviations: py, pyrite; sphal, sphalerite; gn, galena; carb, carbonates; cc, calcite; dol, dolomite; jasp, jasper; qz, quartz; sulph, sulphides; tetra-tenn, tetrahedrite-tennantite; fg, fine-grained; cg, coarse-grained; dolo, dolostone; agg, aggregate; diss, disseminated; Fm, formation; spl, sample, MVT, Mississippi Valley-type; SRS, stratabound replacement sulphides.

** not included in average

Appendix 2. Sulphur isotope compositions and per mil mineral fractionations, Prairie Creek deposit, NT.

Sample / LSI number	$\delta^{34}S_{py}$	σ	$\delta^{34}S_{sphal}$	σ	$\delta^{34}S_{gn}$	σ	$\Delta^{34}S_{py\text{-}sphal}$	T°C**	$\Delta^{34}S_{py\text{-}gn}$	T°C	$\Delta^{34}S_{sph\text{-}gn}$	T°C
PC01-130-313.5 / LSI-S-05-09-01	26.88		25.06				1.82	132				
Stratabound replacement sulphides in OSw3-2	24.45		23.11				1.34	199				
	24.00						*-0.08*	*ne*				
	24.72						*0.64*	*400*				
	26.08						*2.00*	*111*				
	26.08						*2.00*	*111*				
	24.05						*-0.03*	*ne*				
Average (Δ and T°C: disequilibrium data excluded):	**25.18**	**1.15**	**24.08**	**1.38**			***1.56***	***165***				
PC04-150-238.6 / LSI-S-05-09-02	24.27		24.79				-0.52	*ne*				
Stratabound replacement sulphides in OSw3-2	23.81		23.58				0.22	894				
	23.42		24.08				-0.66	*ne*				
	22.77		23.46				-0.69	*ne*				
	23.81		24.73				-0.93	*ne*				
			22.04				*1.58*	*162*				
			22.27				*1.35*	*198*				
			22.94				*0.68*	*390*				
			24.45				*-0.83*	ne				
			23.47				*0.15*	*1140*				
Average (Δ and T°C: disequilibrium data excluded):	**23.62**	**0.56**	**23.34**	**1.02**			***0.22***	***250***				
PC92-16-310.6 / LSI-S-05-09-03	21.32		21.27				0.05	*ne*				
Stratabound replacement sulphides in OSw3-2	22.05		22.67				-0.62	*ne*				
	22.31		22.50				-0.19	*ne*				
	22.94		22.71				0.24	*ne*				
	21.03		22.34				-1.31	*ne*				
	22.51						*0.21*					
Average (Δ and T°C: disequilibrium data excluded):	**22.47**	**1.63**	**22.30**	**0.59**			**0.23**	***ne***				
PC92-19-289.7 / LSI-05-09-04	23.73		18.44		18.76		5.30	*ne*	4.97	197	-0.32	*ne*
Stratabound replacement sulphides in OSw3-2	21.67		19.25		18.53		2.42	*78*	3.14	318	0.72	*ne*
	21.08		18.57		16.89		2.51	*72*	4.19	239	1.68	416
	21.12		21.06		16.34		0.06	*ne*	4.78	206	4.72	138
	21.47		20.46				1.01	*271*	3.84	261	*2.83*	253
	21.55		21.76				-0.21	*ne*	*-1.83*	ne	*4.13*	166
	21.98		20.80				1.18	*230*	*-1.40*	ne	*3.17*	229
	21.38		19.88				1.50	*173*	*-2.00*	ne	*2.25*	323
	21.47						*1.44*	*183*		ne		*ne*
Average (Δ and T°C: disequilibrium data excluded):	**21.72**	**0.80**	**20.03**	**1.20**	**17.63**	**1.20**	**1.72**	***148***	**4.18**	**239**	**3.42**	**210**
PC93-25-251.9 / LSI-05-09-05	24.04		23.42		19.51		0.62	*422*	4.53	219	3.92	178
Stratabound replacement sulphides in OSw3-2	24.17		22.96		19.90		1.21	*224*	4.27	234	3.06	238
	23.88		23.31		19.56		0.57	*452*	4.32	231	3.75	188
	24.24		23.85		19.66		0.39	*603*	4.59	216	4.20	163
	24.43		22.86				1.57	*155*	4.78	206	*3.21*	226
	24.48						*1.20*	*226*	*4.83*	203	*4.83*	133
	24.56						*1.28*	*210*	*4.91*	199	*4.91*	130
	24.50						*1.22*	*222*	*4.85*	202	*4.85*	132
	24.00						*0.72*	*372*	*4.35*	229	*4.35*	155
	24.25						*0.97*	*282*	*4.60*	215	*4.60*	143
Average (Δ and T°C: disequilibrium data excluded):	**24.25**	**0.24**	**23.28**	**0.40**	**19.65**	**0.17**	**0.97**	***282***	**4.60**	**215**	**4.17**	**164**

Appendix 2. Continued.

Sample / LSI number	$\delta^{34}S_{py}$	σ	$\delta^{34}S_{sphal}$	σ	$\delta^{34}S_{gn}$	σ	$\Delta^{34}S_{py\text{-}sphal}$	T°C**	$\Delta^{34}S_{py\text{-}gn}$	T°C	$\Delta^{34}S_{sph\text{-}gn}$	T°C
PC93-24-257.1 / LSI-S-05-09-06	23.65		23.56		15.36		0.09	*ne*	8.29	90	8.20	*39*
Stratabound replacement sulphides in OSw3-2	23.23		22.57		14.26		0.66	400	8.97	76	8.31	37
	23.34		23.33		10.76		0.01	*ne*	12.57	*ne*	12.57	*ne*
	23.21		22.44		12.57		0.77	350	10.64	*ne*	9.87	*ne*
	23.53		24.78		17.96		-1.25	*ne*	5.57	170	6.82	*69*
	23.65		22.49		15.63		1.16	235	8.02	97	6.86	68
	23.51		22.16		20.38		1.35	198	3.13	319	1.78	397
	24.50		22.94		16.03		1.57	163	8.47	87	6.90	*ne*
	23.60		24.05		10.80		-0.45	*ne*	12.80	*ne*	13.25	*ne*
			22.48				*1.10*	*249*			*7.80*	*47*
			23.87				*-0.29*	*ne*			*9.19*	*ne*
			23.03				*0.55*	*465*			*8.35*	*ne*
			23.52				*0.06*	*ne*			*8.84*	*ne*
			20.80				*2.78*	*70*			*6.12*	*88*
			21.06				*2.53*	*70*			*6.38*	*ne*
			23.89				*-0.31*	*ne*			*9.21*	*ne*
			22.03				*1.55*	166			*7.35*	*ne*
			22.65				*0.93*	294			*7.97*	*ne*
			23.14				*0.44*	*552*			*8.46*	*ne*
Average (Δ and T°C: disequilibrium data excluded):	**23.58**	**0.39**	**22.88**	**1.20**	**14.86**	**3.19**	**1.28**	**210**	**7.08**	**120**	**6.56**	**75**
PC93-35-224.8 / LSI-S-05-09-07	24.30		21.98				*ne*	86				
Stratabound replacement sulphides in OSw3-2	22.99		22.99				*ne*	*ne*				
	23.34		21.34				2.00	114				
	23.51		20.60				2.91	*ne*				
	22.35		21.68				0.67	395				
			21.20				*2.10*	*104*				
			21.36				*1.94*	*119*				
			21.76				*1.55*	*166*				
Average (Δ and T°C: disequilibrium data excluded):	**23.30**	**0.71**	**21.61**	**0.70**			**1.90**	**124**				
PC93-41-246.7 / LSI-05-09-08	21.79		23.86		15.81		-2.07	*ne*	5.97	*ne*	8.05	*ne*
Stratabound replacement sulphides in OSw3-4	20.36		22.42		15.18		-2.06	*ne*	5.18	*ne*	7.24	*ne*
	23.28		17.55		14.62		5.73	*ne*	8.66	*ne*	2.93	*ne*
	23.56		20.37				3.20	*ne*	*8.35*	*ne*	*5.16*	120
			20.18				*2.07*	*107*			*4.97*	128
			21.47				*0.78*	*346*			*6.26*	84
			23.11				*-0.86*	*ne*			*7.90*	*ne*
			23.01				*-0.76*	*ne*			*7.80*	*ne*
			22.36				*-0.11*	*ne*			*7.15*	*ne*
			21.07				*1.18*	*230*			*5.86*	*ne*
			22.72				*-0.47*	*ne*			*7.51*	*ne*
			24.22				*-1.97*	*ne*			*9.01*	*ne*
			22.53				*-0.28*	*ne*			*7.32*	*ne*
			23.16				*-0.91*	*ne*			*7.95*	*ne*
Average (Δ and T°C: disequilibrium data excluded):	**22.25**	**1.48**	**22.00**	**1.75**	**15.21**	**0.60**	**1.34**	*199*	**7.04**	121	**5.06**	124
PC94-64-207.6 / LSI-S-05-09-09	16.64		22.91		18.94		-0.31	*ne*	-2.30	*ne*	3.96	176
Stratabound replacement sulphides in OSw3-6	22.85		22.34		19.04		0.26	493	3.81	264	3.30	219
	21.12		21.46		19.96		1.14	*ne*	1.17	117	1.51	454

Appendix 2. Continued.

Sample / LSI number	$\delta^{34}S_{py}$	σ	$\delta^{34}S_{sphal}$	σ	$\delta^{34}S_{gn}$	σ	$\Delta^{34}S_{py\text{-}sphal}$	T°C**	$\Delta^{34}S_{py\text{-}gn}$	T°C	$\Delta^{34}S_{sph\text{-}gn}$	T°C
	23.81		21.01		20.05		1.60	53	3.76	267	0.95	*ne*
			23.14		19.71		*-2.03*	*ne*	*3.60*	*279*	3.43	209
			23.00				*-1.89*	*ne*	*3.46*	*290*	*3.46*	207
			20.28				*0.84*	324	*0.73*	*ne*	*0.73*	*ne*
			20.86				*0.25*	*ne*	*1.32*	*ne*	*1.32*	505
			21.07				*0.04*	*ne*	*1.53*	*ne*	*1.53*	449
Average (Δ and T°C: disequilibrium data excluded):	**22.60**	**1.36**	**21.78**	**1.07**	**19.54**	**0.52**	**1.19**	**228**	**3.16**	**316**	**2.83**	**258**
PC94-75-204.5 / LSI-S-05-09-10	14.92											
Mississippi Valley-type (MVT) sulph	14.74											
in Root River Fm.	14.74											
	15.94											
	15.94											
	12.91											
	15.41											
	17.09											
Average (Δ and T°C: disequilibrium data excluded):	**15.21**	**1.22**										
PC94-82-496.1 / LSI-05-09-11	23.71		22.84		21.78		0.87	313	1.93	481	1.06	176
Stratabound replacement sulphides in OSw3-4	24.88				19.27		*2.04*	109	5.61	169	3.58	199
	24.56				17.32		*1.72*	144	7.24	*ne*	5.52	107
	24.79				20.45		*1.95*	119	4.33	230	2.39	405
	24.43						*1.59*	160	5.16	188		
	25.19						*2.35*	83	5.92	157		
	24.85						*2.01*	113	5.58	170		
Average (Δ and T°C: disequilibrium data excluded):	**24.63**	**0.47**	**22.84**		**19.71**	**1.89**	**1.79**	**136**	**5.32**	**181**	**3.14**	**231**
PC95-97-79.1 / LSI-05-09-12	22.88				3.06				19.82	*ne*		
Stratabound replacement sulph in OSw3-2	22.76				3.96				18.80	*ne*		
	20.03								*16.52*	*ne*		
	23.69								*20.18*	*ne*		
	21.59								*18.08*	*ne*		
	23.61								*20.10*	*ne*		
	23.55								*20.04*	*ne*		
Average (Δ and T°C: disequilibrium data excluded):	**22.59**	**1.34**			**3.51**	**0.64**			**19.31**	*ne*		
PC95-125-760 / LSI-S-05-09-13					19.59							
Quartz-carbonate-sulph vein in Road River Fm					19.67							
					21.65							
					20.45							
					20.07							
					20.28	**0.84**						
PC93-23-249.7 / LSI-S-05-09-14	23.53		24.60		22.62		-1.07	*ne*	0.91	*ne*	1.98	362
Stratabound replacement sulphides in OSw3-2	22.90		24.58		21.75		*-1.05*	*ne*	*1.47*	*ne*	2.83	258
			25.18		20.14		*-1.65*	*ne*	*3.08*	*324*	5.04	125
					19.99				*3.23*	*310*	4.79	135
Average (Δ and T°C: disequilibrium data excluded):	**23.22**		**24.78**	**0.34**	**21.13**	**1.27**			**3.47**	**317**	**3.66**	**220**

** Isotopic equilibration temperatures based on Kajiwara and Krouse (1971)

NOTE: "ne" indicates a clear instance of non-equilibrium